NATIONAL ADVISORY COMMITTEE FOR AERONAUTICS

REPORT No. 650

THE AERODYNAMIC CHARACTERISTICS OF SIX FULL-SCALE PROPELLERS HAVING DIFFERENT AIRFOIL SECTIONS

By DAVID BIERMANN and EDWIN P. HARTMAN

1939

For sale by the Superintendent of Documents, Washington, D. C. - - - - - - - - - - - - - - - Price 10 cents
(Subscription price $3 per year)

AERONAUTIC SYMBOLS

1. FUNDAMENTAL AND DERIVED UNITS

	Symbol	Metric		English	
		Unit	Abbreviation	Unit	Abbreviation
Length	l	meter	m	foot (or mile)	ft. (or mi.)
Time	t	second	s	second (or hour)	sec. (or hr.)
Force	F	weight of 1 kilogram	kg	weight of 1 pound	lb.
Power	P	horsepower (metric)		horsepower	hp.
Speed	V	kilometers per hour	k.p.h.	miles per hour	m.p.h.
		meters per second	m.p.s.	feet per second	f.p.s.

2. GENERAL SYMBOLS

W, Weight $=mg$

g, Standard acceleration of gravity $=9.80665$ m/s^2 or 32.1740 ft./sec.^{2}

m, Mass $=\frac{W}{g}$

I, Moment of inertia $=mk^2$. (Indicate axis of radius of gyration k by proper subscript.)

μ, Coefficient of viscosity

ν, Kinematic viscosity

ρ, Density (mass per unit volume)

Standard density of dry air, 0.12497 kg-m^{-4}-s^2 at 15° C. and 760 mm; or 0.002378 lb.-ft.$^{-4}$ sec.^{2}

Specific weight of "standard" air, 1.2255 kg/m^3 or 0.07651 lb./cu. ft.

3. AERODYNAMIC SYMBOLS

S, Area

S_w, Area of wing

G, Gap

b, Span

c, Chord

$\frac{b^2}{S}$, Aspect ratio

V, True air speed

q, Dynamic pressure $=\frac{1}{2}\rho V^2$

L, Lift, absolute coefficient $C_L=\frac{L}{qS}$

D, Drag, absolute coefficient $C_D=\frac{D}{qS}$

D_0, Profile drag, absolute coefficient $C_{D_0}=\frac{D_0}{qS}$

D_i, Induced drag, absolute coefficient $C_{D_i}=\frac{D_i}{qS}$

D_p, Parasite drag, absolute coefficient $C_{D_p}=\frac{D_p}{qS}$

C, Cross-wind force, absolute coefficient $C_C=\frac{C}{qS}$

R, Resultant force

i_w, Angle of setting of wings (relative to thrust line)

i_t, Angle of stabilizer setting (relative to thrust line)

Q, Resultant moment

Ω, Resultant angular velocity

$\rho\frac{Vl}{\mu}$, Reynolds Number, where l is a linear dimension (e.g., for a model airfoil 3 in. chord, 100 m.p.h. normal pressure at 15° C., the corresponding number is 234,000; or for a model of 10 cm chord, 40 m.p.s., the corresponding number is 274,000)

C_p, Center-of-pressure coefficient (ratio of distance of c.p. from leading edge to chord length)

α, Angle of attack

ϵ, Angle of downwash

α_0, Angle of attack, infinite aspect ratio

α_i, Angle of attack, induced

α_a, Angle of attack, absolute (measured from zero-lift position)

γ, Flight-path angle

REPORT No. 650

THE AERODYNAMIC CHARACTERISTICS OF SIX FULL-SCALE PROPELLERS HAVING DIFFERENT AIRFOIL SECTIONS

By DAVID BIERMANN and EDWIN P. HARTMAN

Langley Memorial Aeronautical Laboratory

130644—39——1

NATIONAL ADVISORY COMMITTEE FOR AERONAUTICS

HEADQUARTERS, NAVY BUILDING, WASHINGTON, D. C.

LABORATORIES, LANGLEY FIELD, VA.

Created by act of Congress approved March 3, 1915, for the supervision and direction of the scientific study of the problems of flight (U. S. Code, Title 50, Sec. 151). Its membership was increased to 15 by act approved March 2, 1929. The members are appointed by the President, and serve as such without compensation.

TECHNICAL COMMITTEES

AERODYNAMICS
POWER PLANTS FOR AIRCRAFT
AIRCRAFT MATERIALS

AIRCRAFT STRUCTURES
AIRCRAFT ACCIDENTS
INVENTIONS AND DESIGNS

Coordination of Research Needs of Military and Civil Aviation

Preparation of Research Programs

Allocation of Problems

Prevention of Duplication

Consideration of Inventions

LANGLEY MEMORIAL AERONAUTICAL LABORATORY

LANGLEY FIELD, VA.

Unified conduct, for all agencies, of scientific research on the fundamental problems of flight.

OFFICE OF AERONAUTICAL INTELLIGENCE

WASHINGTON, D. C.

Collection, classification, compilation, and dissemination of scientific and technical information on aeronautics.

5-24-39

REPORT No. 650

THE AERODYNAMIC CHARACTERISTICS OF SIX FULL-SCALE PROPELLERS HAVING DIFFERENT AIRFOIL SECTIONS

By David Biermann and Edwin P. Hartman

SUMMARY

Wind-tunnel tests are reported of six 3-blade 10-foot propellers operated in front of a liquid-cooled engine nacelle. The propellers were identical except for blade airfoil sections, which were: Clark Y, R. A. F. 6, N. A. C. A. 4400, N. A. C. A. 2400 34, N. A. C. A. 2R$_2$00, and N. A. C. A. 6400. The range of blade angles investigated extended from 15° to 40° for all propellers except the Clark Y, for which it extended to 45°.

The results showed that the range in maximum efficiency between the highest and the lowest values was about 3 percent. The highest efficiencies were for the low-camber sections. An analysis of the results indicated that blade sections for controllable propellers which are not limited in diameter should be selected chiefly on a basis of minimum drag (which affects maximum efficiency) inasmuch as the maximum lift coefficients had only a small effect on the take-off characteristics within the range investigated because stalling, in general, did not occur. Sections for fixed-pitch propellers should be selected on a basis of both minimum drag and maximum lift, particularly for blade-angle settings of 20° and over, because the take-off thrust power increased with maximum lift for the higher blade angles.

INTRODUCTION

The Clark Y and the R. A. F. 6 airfoil sections have been standard in the design of propellers in this country for many years. The R. A. F. 6 section was favored in early designs but has given way to the Clark Y section more recently, particularly for metal controllable propellers. The relative merits of the two sections for propeller use have been fairly well established by both high-speed airfoil and full-scale propeller tests. The airfoil tests reported in reference 1 showed the Clark Y section to have a lower minimum drag and a lower maximum lift than the R. A. F. 6 section, which indicates that a propeller with the Clark Y section would be superior for the high-speed or cruising conditions but inferior for take-off with fixed-pitch propellers. The propeller results of reference 2 qualitatively substantiate the airfoil results. The principal physical difference between the two sections is the shape of the mean camber lines; the camber line of the R. A. F. 6 section is higher than that of the Clark Y, particularly for the nose parts of the sections.

The present investigation was made to determine the aerodynamic qualities of six propellers having different sections. The Clark Y and the R. A. F. 6 sections were included for comparative purposes. Two of the other propellers were designed by the Bureau of Aeronautics, Navy Department; the N. A. C. A. 4400 series section was used for one, and the N. A. C. A. 4400 series section was used for the inner half of the other, the N. A. C. A. 2400–34 series section being used for the outer half. It may be noted in reference 3 that the N. A. C. A. 4409 section (used at 0.75 propeller radius) has a high $C_{L_{max}}$ and a fairly low $C_{D_{min}}$ and is therefore a good compromise between the Clark Y and the R. A. F. 6 sections. In reference 4 the N. A. C. A. 2409–34 section is recommended for propellers, particularly because of its low $C_{D_{min}}$ and delayed compressibility stall at high speeds. The section is best suited for only the tip sections of propellers, however, because the $C_{L_{max}}$ is low at moderate speeds.

In addition to the four propellers described, there were designed at the N. A. C. A. laboratory two additional propellers that incorporated sections of extreme characteristics. One propeller has sections of the low-camber N. A. C. A. 2R$_2$00 series, which has a low $C_{D_{min}}$ and a low $C_{L_{max}}$; the other propeller has the high-camber N. A. C. A. 6400 series section, which has a high $C_{D_{min}}$ and a high $C_{L_{max}}$. (See reference 3.) Tests of these propellers were added to the program to increase the known range of the propeller characteristics that are dependent upon the amount of section camber present.

APPARATUS AND METHODS

Since the description of reference 5 was written, the propeller-research tunnel has been modified to the extent of installing an electric motor to drive the tunnel propeller and of replacing the balance with a more

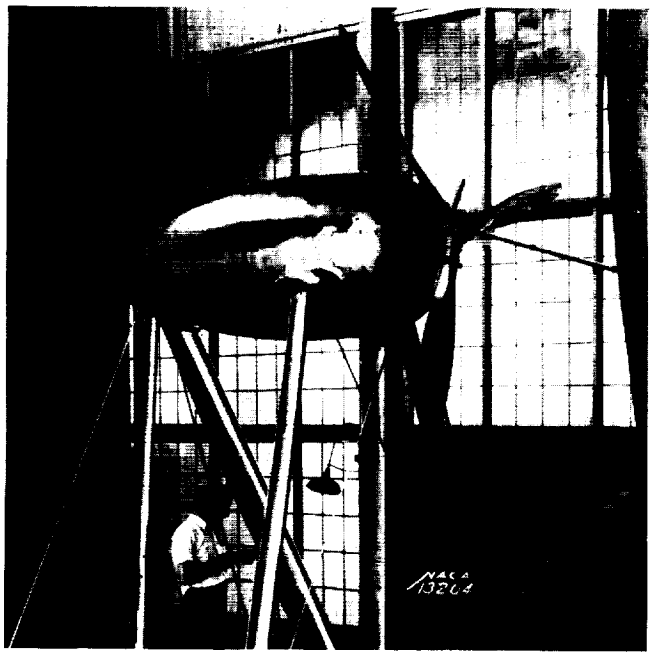

FIGURE 1.—Liquid-cooled engine nacelle.

modern one capable of simultaneously recording all the forces.

A 600-horsepower Curtiss Conqueror engine (GIV–1570) was used to drive the test propellers. The engine was mounted in a cradle dynamometer free to rotate about an axis parallel to the propeller axis and

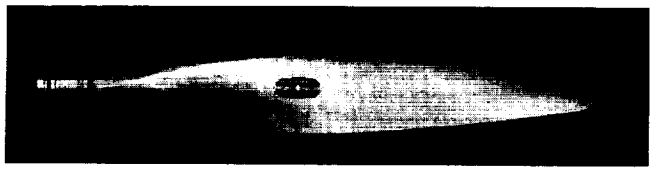

FIGURE 2.—Photograph showing the plan form of all the propellers tested.

located at one side of the engine. The torque reaction was transmitted from the other side of the engine to recording scales located on the floor of the test chamber. The propeller speed was measured by a calibrated electric tachometer.

The engine was housed in a nacelle representative of the type used for liquid-cooled engines. (See fig. 1.) The nacelle is oval in cross section, 43 inches in height, 38 inches in width, and 126 inches in length. A scale drawing of the nacelle is given in reference 6.

All six propellers tested have three blades, are 10 feet in diameter, and are identical in shape except for blade sections. Table I gives the principal physical characteristics of the propellers tested.

TABLE I

Propeller (Bureau of Aeronautics, Navy Department drawing No.)	Blade airfoil section	Camber (percent chord)	Position of maximum camber (percent chord)
5868–9	Clark Y	[1] 2.6	40
5868–R6	R. A. F. 6	[1] 4.0	30
6623–A	N. A. C. A. 4400 series	4.0	40
6623–B	N. A. C. A. 4400 series inner half.	4.0	40
	N. A. C. A. 2400–34 series outer half.	2.0	
6623–C	N. A. C. A. 2R200	2.0	30
6623–D	N. A. C. A. 6400	6.0	40

[1] For the 0.75 radius station only.

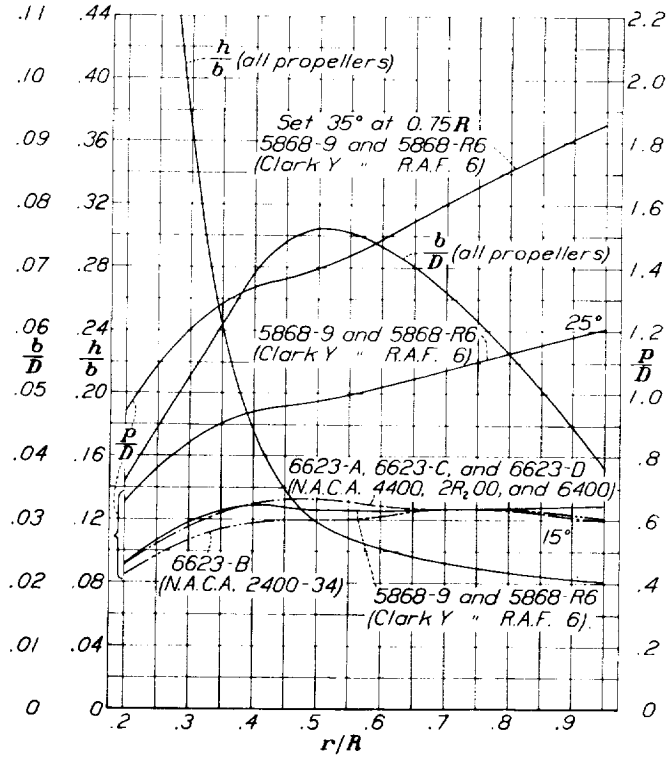

FIGURE 3.—Blade-form curves for all propellers tested. D, diameter; R, radius to the tip; r, station radius; b, section chord; h, section thickness; p, geometric pitch.

Throughout this report, the propellers will be individually referred to according to their sections or grouped according to camber ratio. Propeller 6623–B, for example, will be designated the N. A. C. A. 2400–34 propeller.

Figure 2 shows the plan form of the blades; the blade-form curves are given in figure 3.

It may be noted that the geometric pitch is different for all of the propellers except for the 5868–9 and the 5868–R6. The propellers of N. A. C. A. section were designed with the blade angle of each section, measured from the angle for zero lift, the same as for propeller 5868–9. As a result of this method of design, all the propellers have the same effective pitch distribution along the blade but, of course, the pitches measured with respect to the chord lines are different.

Ordinates for the Clark Y and the R. A. F. 6 propeller sections are given in table II and those for the four propellers with the N. A. C. A. sections are given in table III. The outlines of each blade section for the 0.70 radius are given in figure 4.

The method of testing in the propeller-research tunnel consists in maintaining the propeller speed constant and increasing the tunnel speed in steps up to the maximum value of 115 miles per hour. Higher values of V/nD are obtained by reducing the engine speed until zero thrust is reached. Complications arising from compressibility were avoided by running the tests at tip speeds of 525 feet per second and less. The standard initial testing propeller speed of 1,000 r. p. m. could not be maintained for the higher blade-angle settings, owing to the limitation of engine power; the following schedule was therefore adhered to:

Propeller speeds for tunnel speeds below 115 miles per hour

Blade angle, deg.	*Initial propeller speed, r. p. m.*
15	1,000
20	1,000
25	800
30	800
35	800
40	700
45	700

For V/nD values higher than can be obtained from the foregoing schedule, the approximate test propeller speed may be computed from the relation

$$\text{r. p. m.} = \frac{K}{V/nD}$$

where $K = 1{,}000$ for $V = 115$ miles per hour and $D = 10$ feet.

RESULTS AND DISCUSSION

The results are reduced to the usual coefficients of thrust, power, and propulsive efficiency defined as:

$$C_T = \frac{\text{effective thrust}}{\rho n^2 D^4} = \frac{T - \Delta D}{\rho n^2 D^4}$$

$$C_P = \frac{\text{engine power}}{\rho n^3 D^5}$$

$$\eta = \frac{C_T}{C_P}\frac{V}{nD}$$

where

T is tension in propeller shaft, pounds.
ΔD, increase in body drag due to slipstream, pounds.
ρ, mass density of the air, slugs per cubic foot.
n, propeller rotational speed, revolutions per second.
D, propeller diameter, feet.

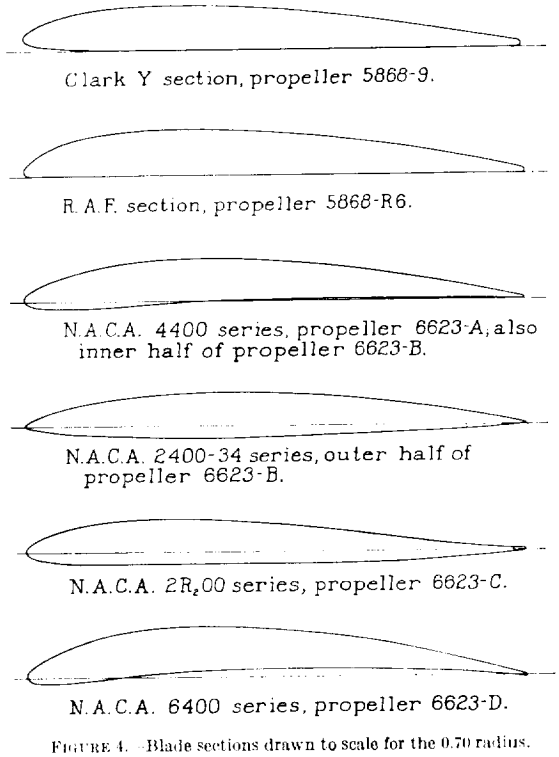

FIGURE 4.—Blade sections drawn to scale for the 0.70 radius.

Charts for selecting or designing propellers are given in the form of C_s against η and V/nD, where $C_s = \sqrt[5]{\rho V^5/Pn^2}$.

The procedure of plotting lines of constant thrust with respect to the power is now standardized and facilitates calculating the thrust at all air speeds for controllable and fixed-pitch propellers. The outline of the method is given in reference 6.

The basic results are presented in the form of curves in figures 5 to 28; comparisons and derived data are given in figures 29 to 42. The test results have been tabulated in six tables and are available on request from the National Advisory Committee for Aeronautics.

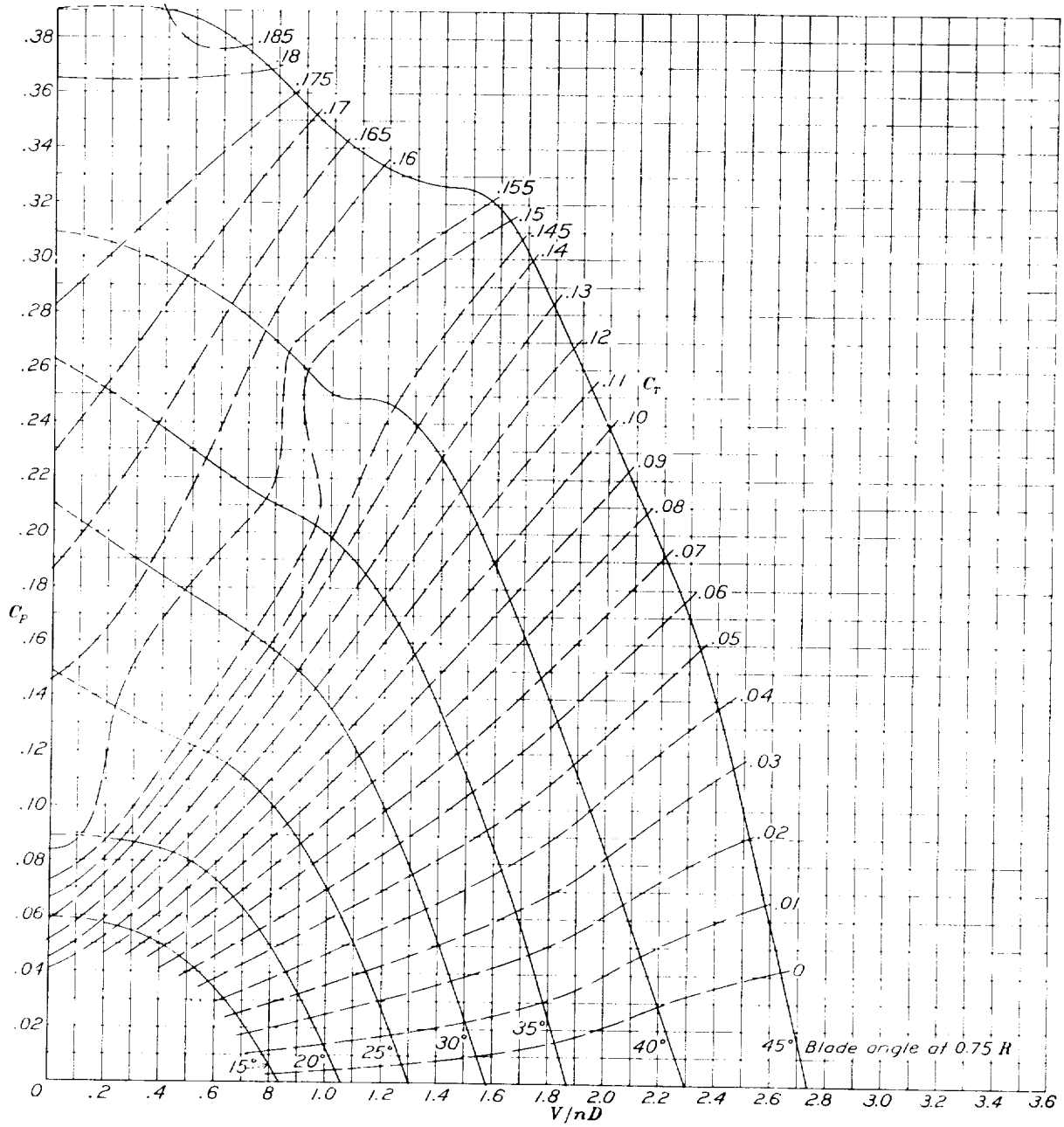

FIGURE 5. Power-coefficient curves for propeller 5868-9 (Clark Y section).

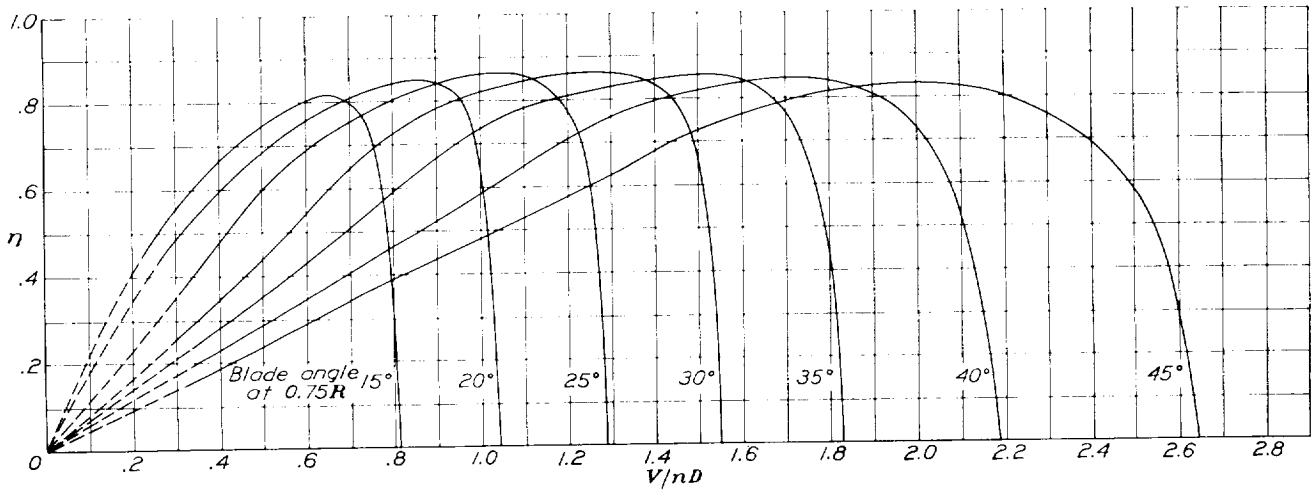

FIGURE 6.—Efficiency curves for propeller 5868-9 (Clark Y section).

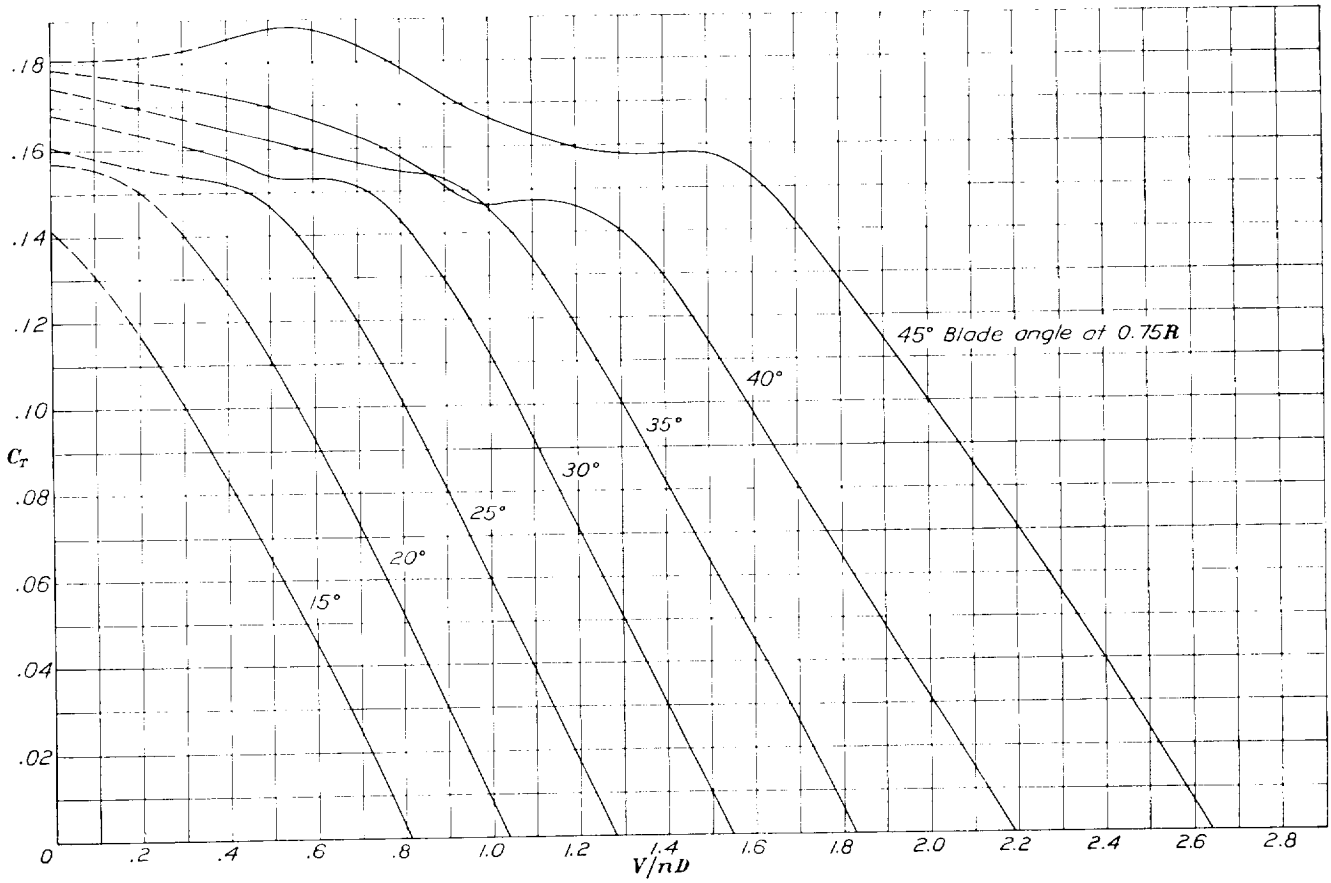

FIGURE 7.—Thrust-coefficient curves for propeller 5868-9 (Clark Y section).

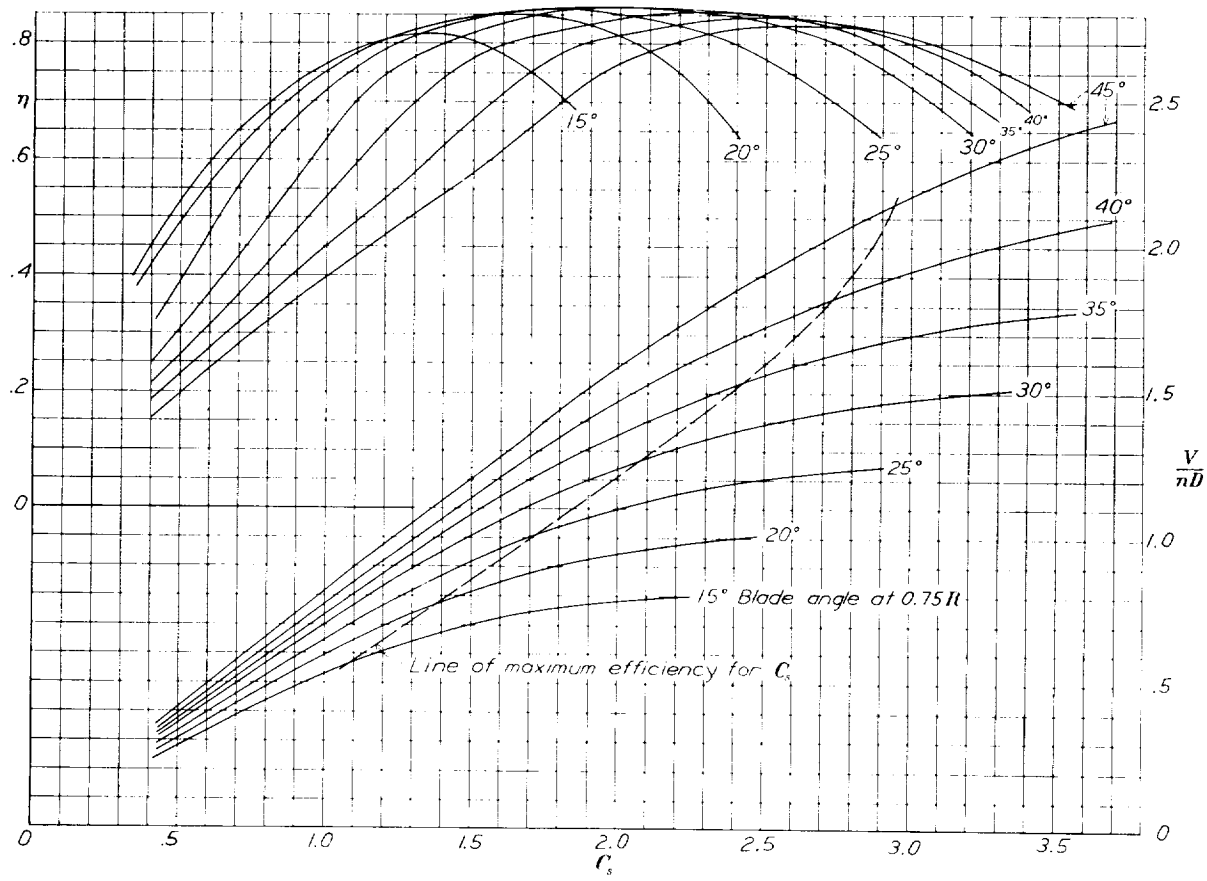

FIGURE 8.—Design chart for propeller 5868-9 (Clark Y section).

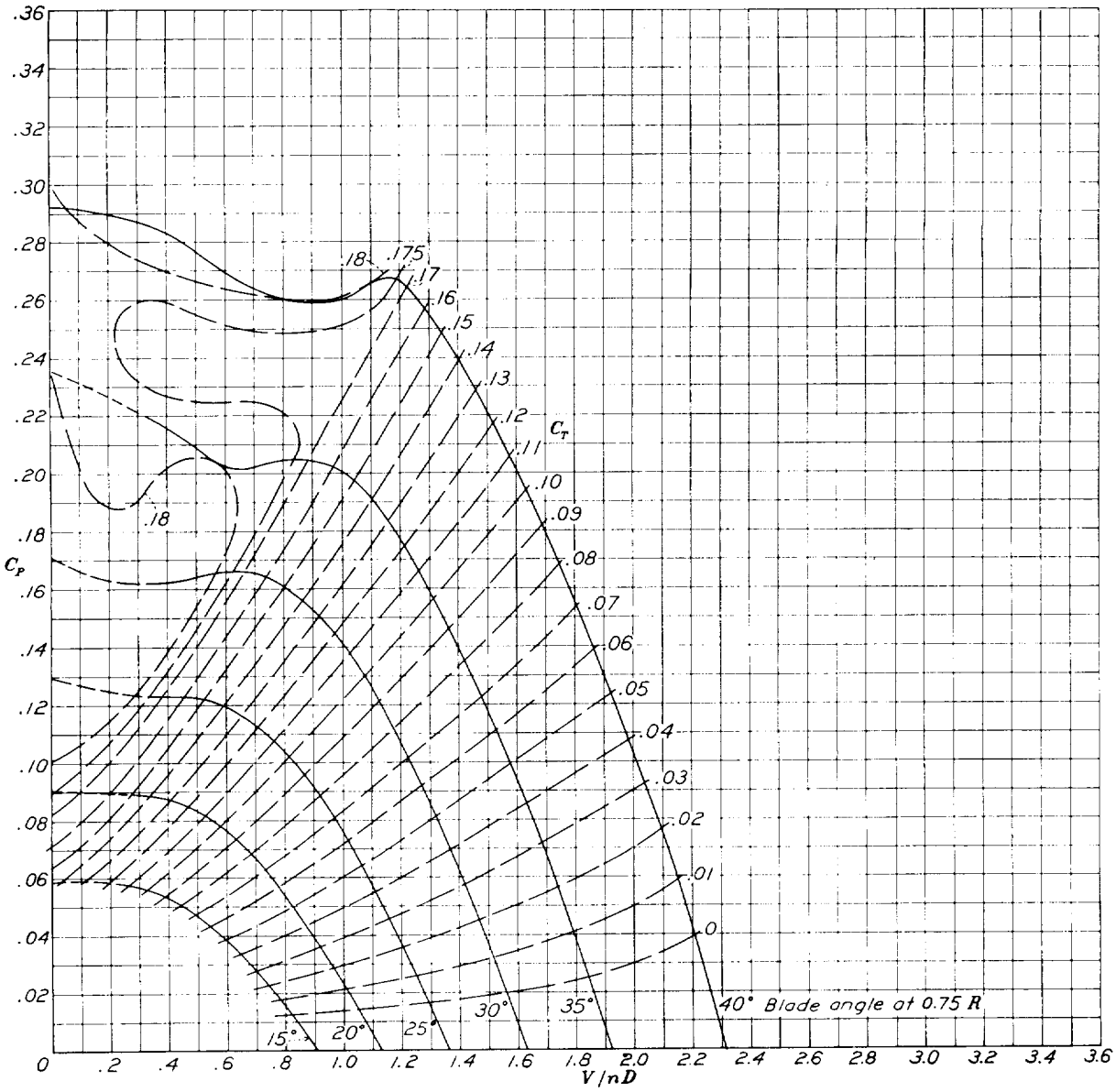

FIGURE 9.—Power-coefficient curves for propeller 5868-R6 (R. A. F. 6 section).

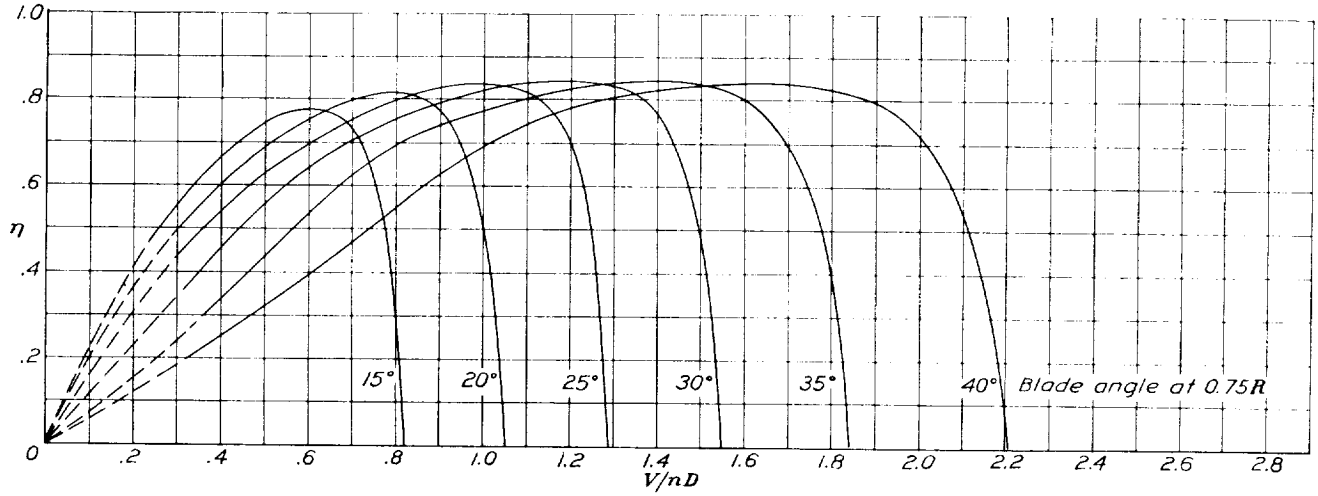

FIGURE 10. Efficiency curves for propeller 5868-R6 (R. A. F. 6 section).

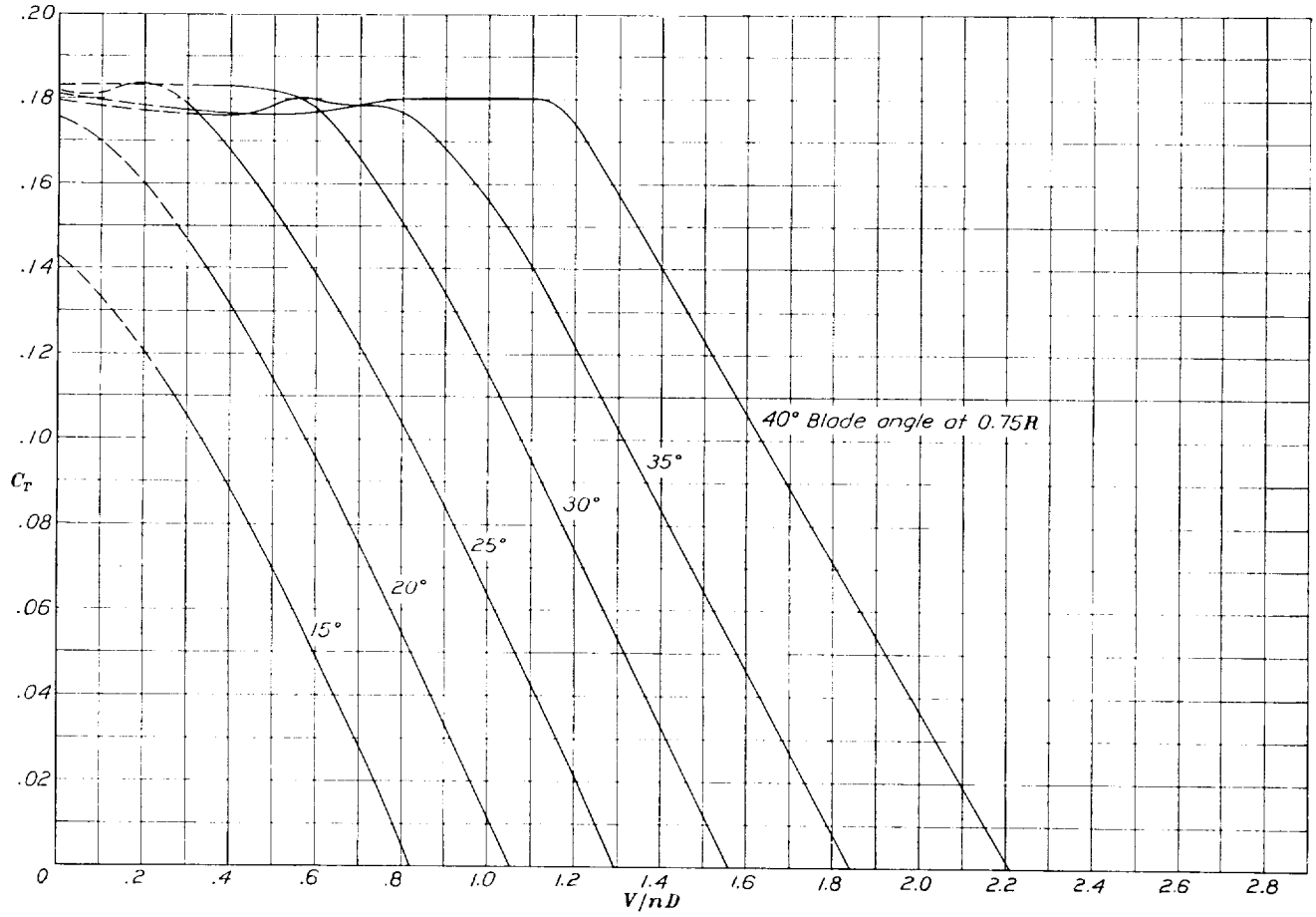

FIGURE 11.—Thrust-coefficient curves for propeller 5868-R6 (R. A. F. 6 section).

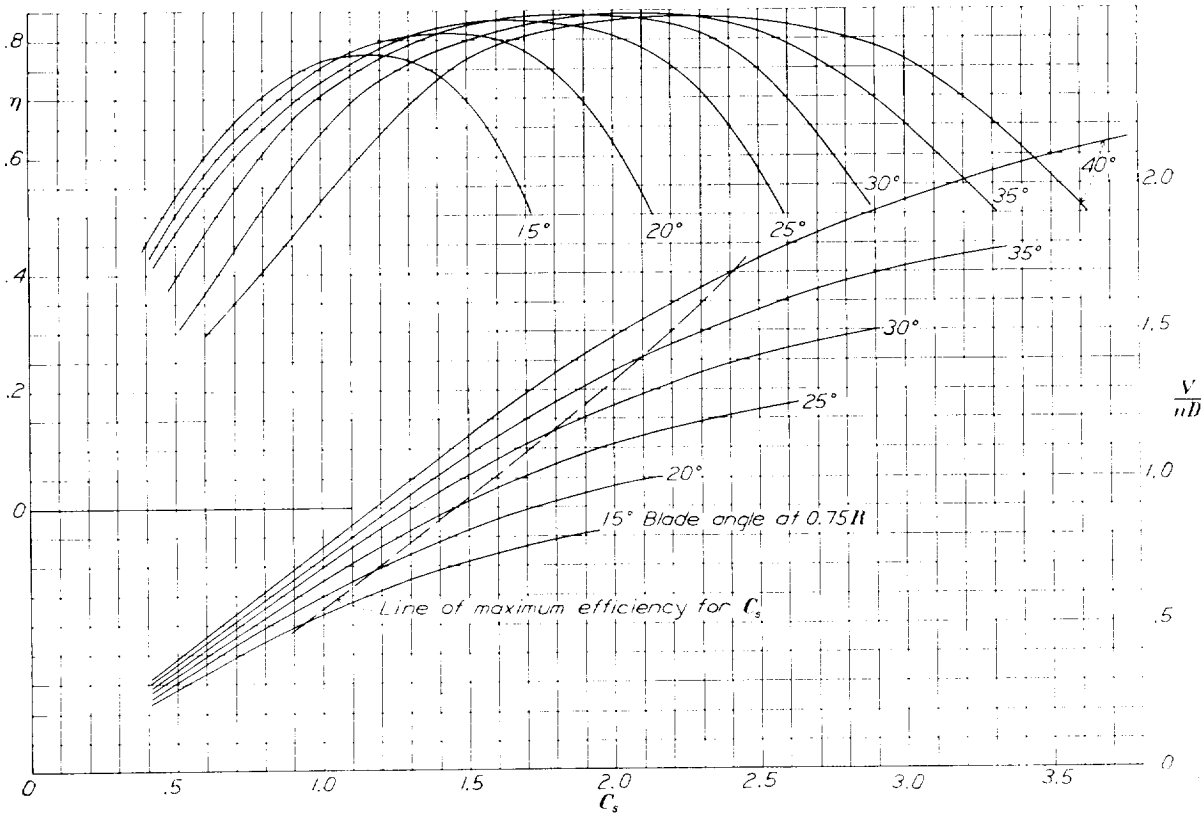

FIGURE 12.—Design chart for propeller 5868–R6 (R. A. F. 6 section).

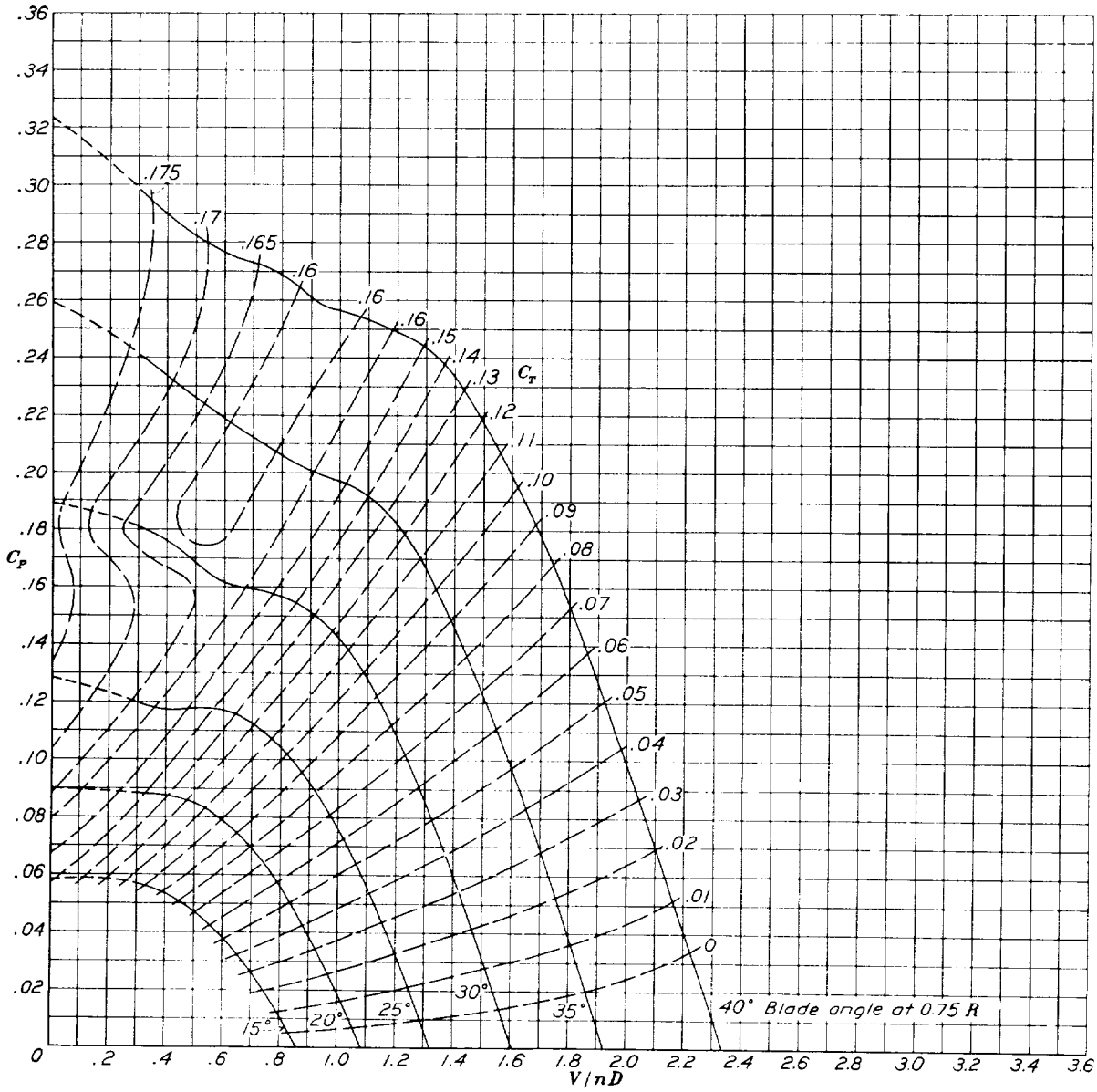

FIGURE 13.—Power-coefficient curves for propeller 6623–A (N. A. C. A. 4400 section).

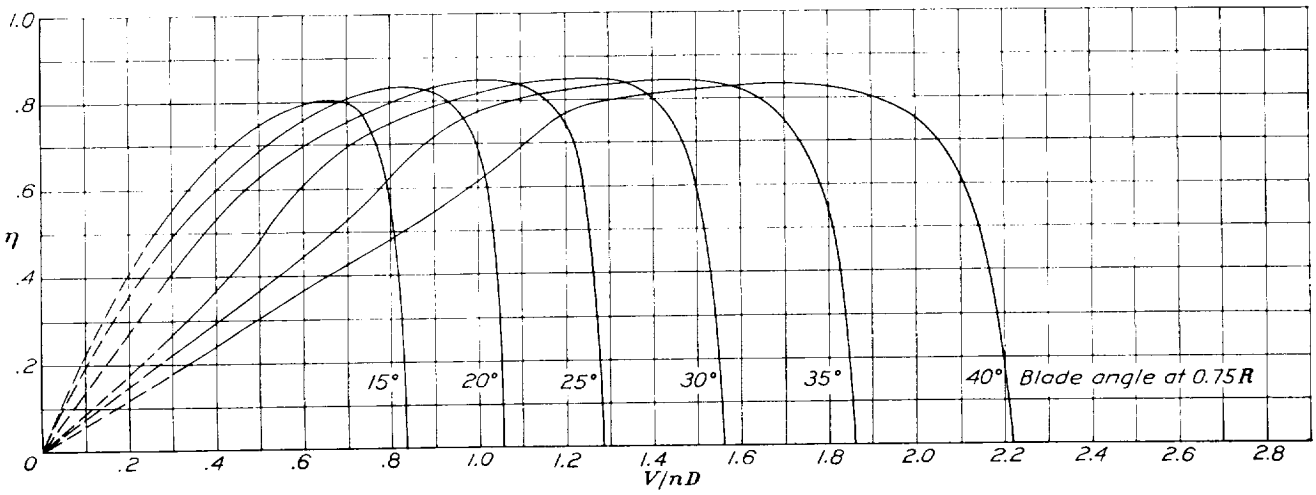

FIGURE 14.- Efficiency curves for propeller 6623-A (N. A. C. A. 4400 section).

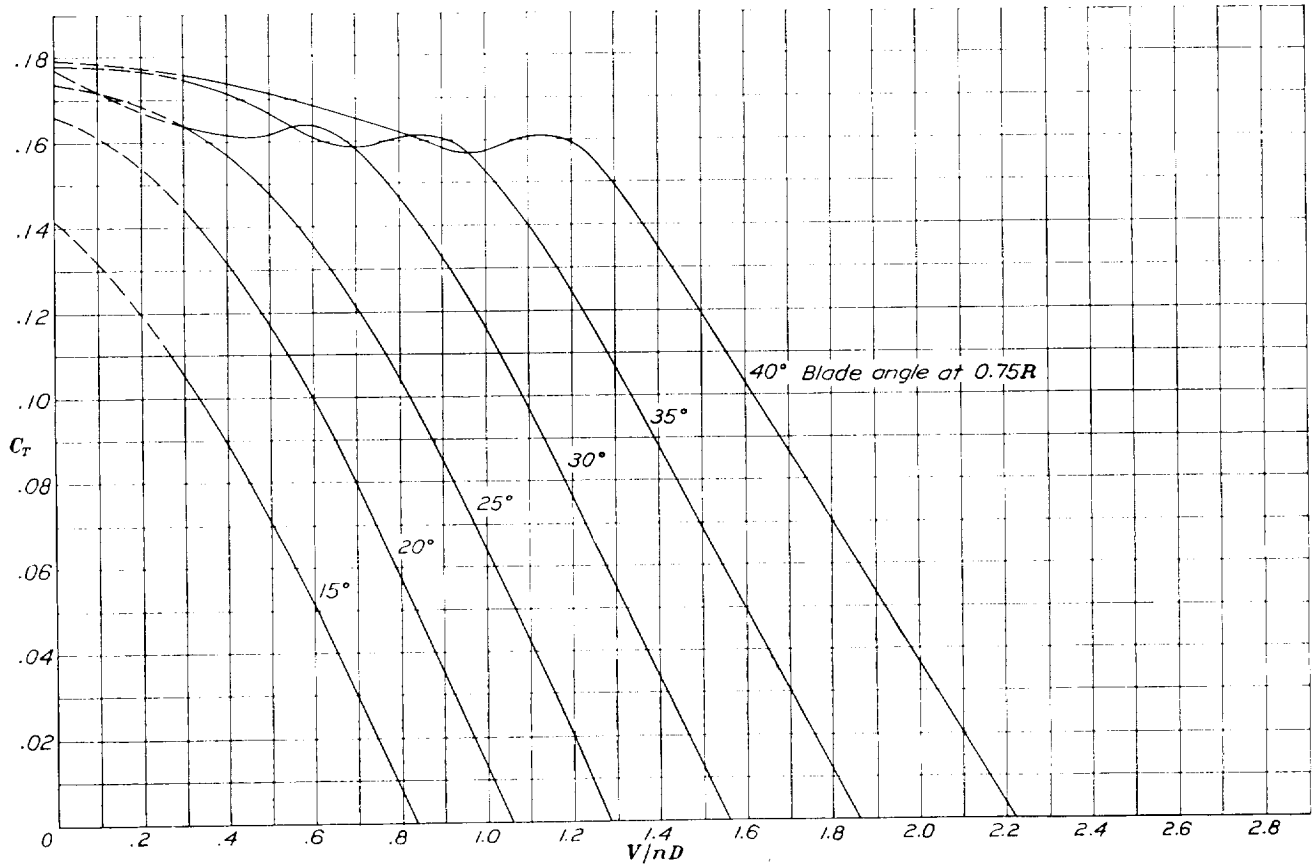

FIGURE 15.- Thrust-coefficient curves for propeller 6623-A (N. A. C. A. 4400 section).

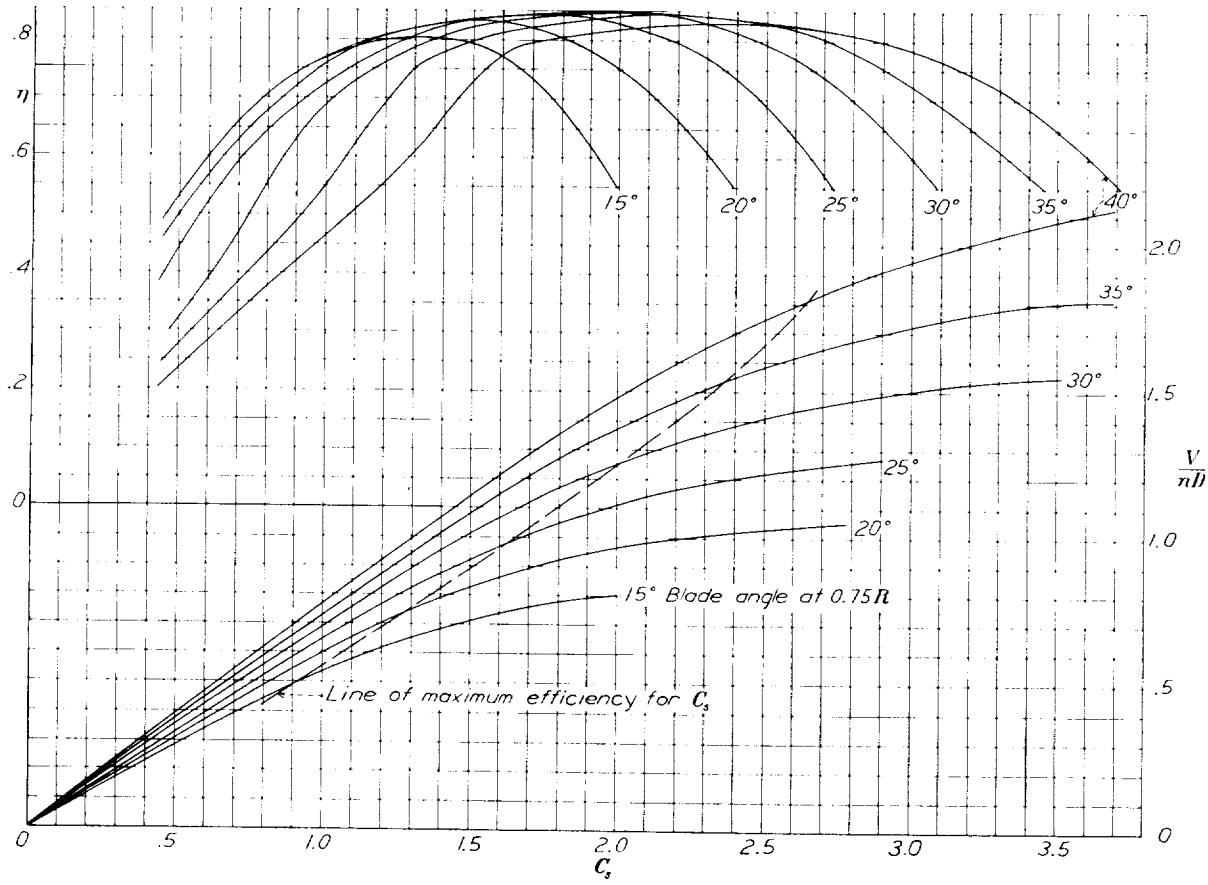

FIGURE 16.—Design chart for propeller 6623-A (N. A. C. A. 4400 section).

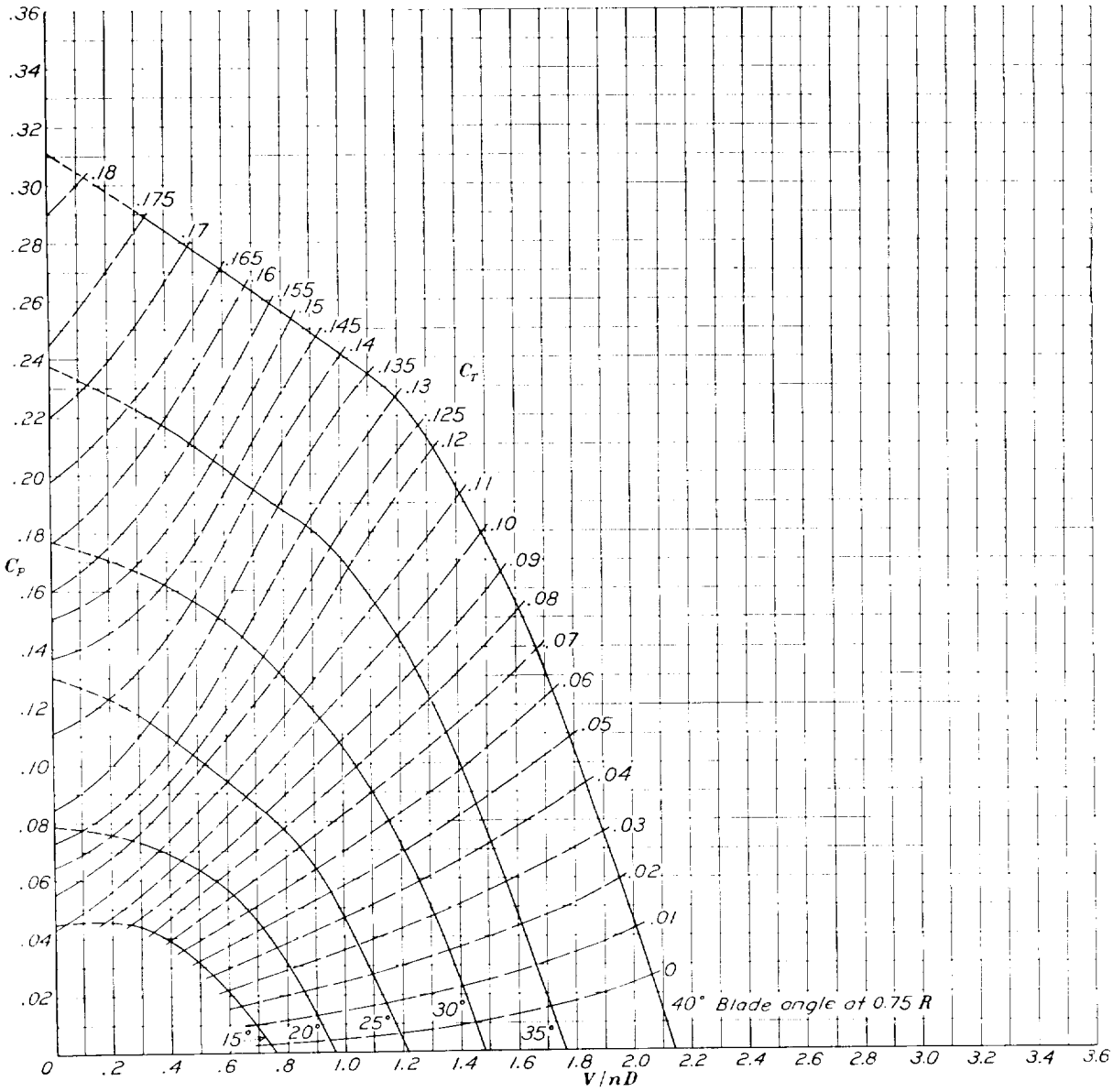

FIGURE 17. Power-coefficient curves for propeller 6623-B (N. A. C. A. 4400 section inner half; N. A. C. A. 2400-34 section outer half).

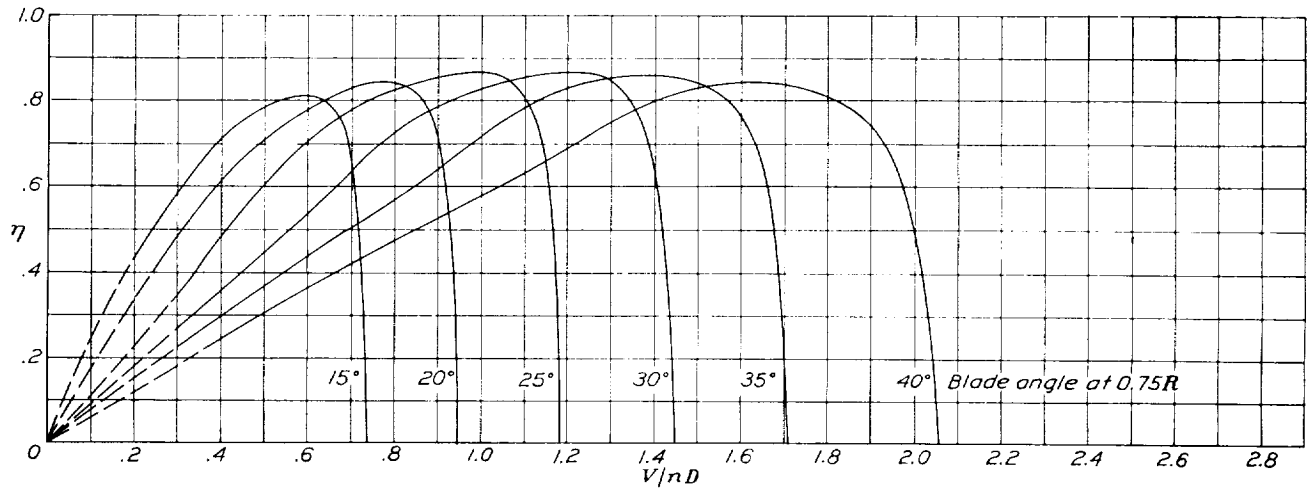

FIGURE 18.—Efficiency curves for propeller 6623-B (N. A. C. A. 4400 section inner half; N. A. C. A. 2400 34 section outer half).

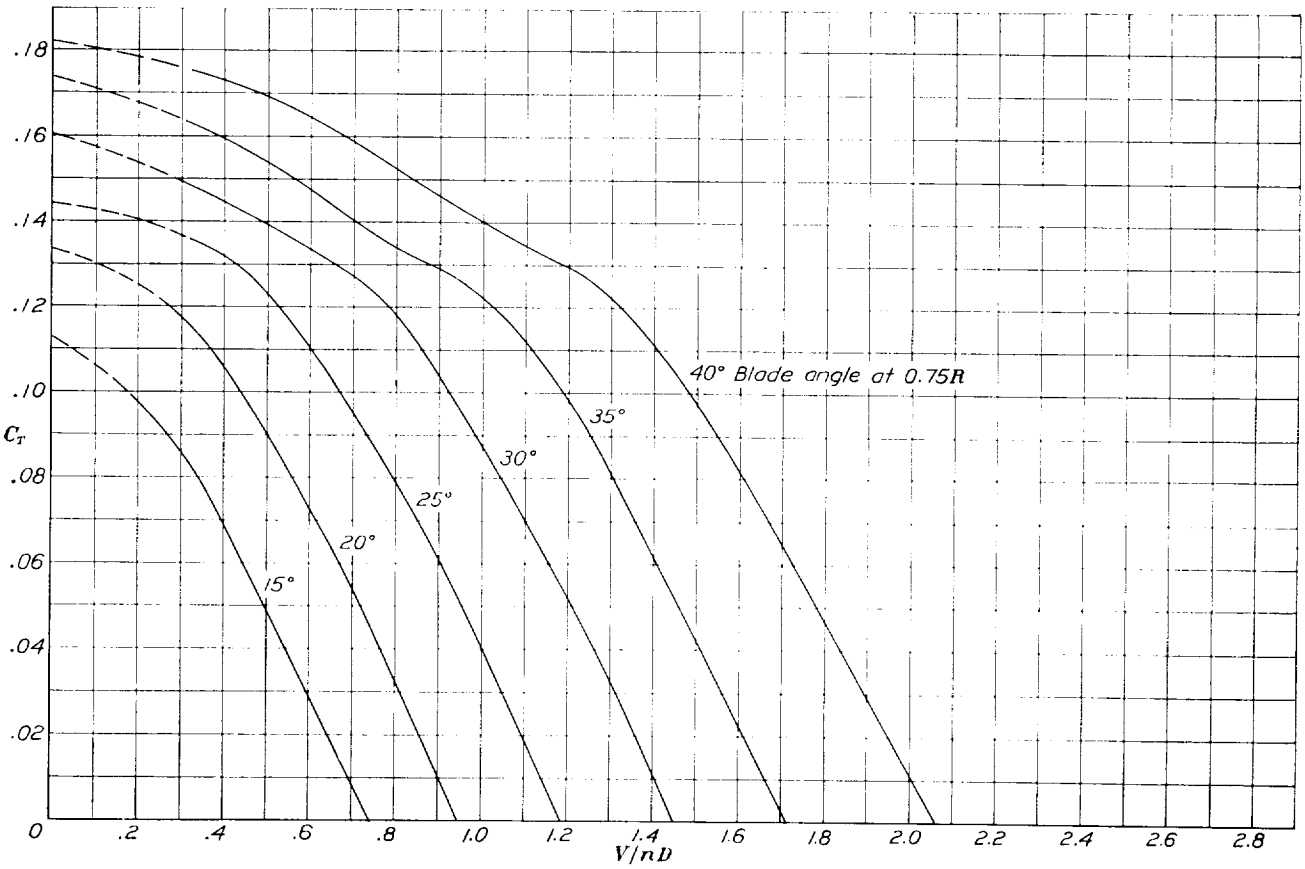

FIGURE 19.—Thrust-coefficient curves for propeller 6623-B (N. A. C. A. 4400 section inner half; N. A. C. A. 2400 34 section route half).

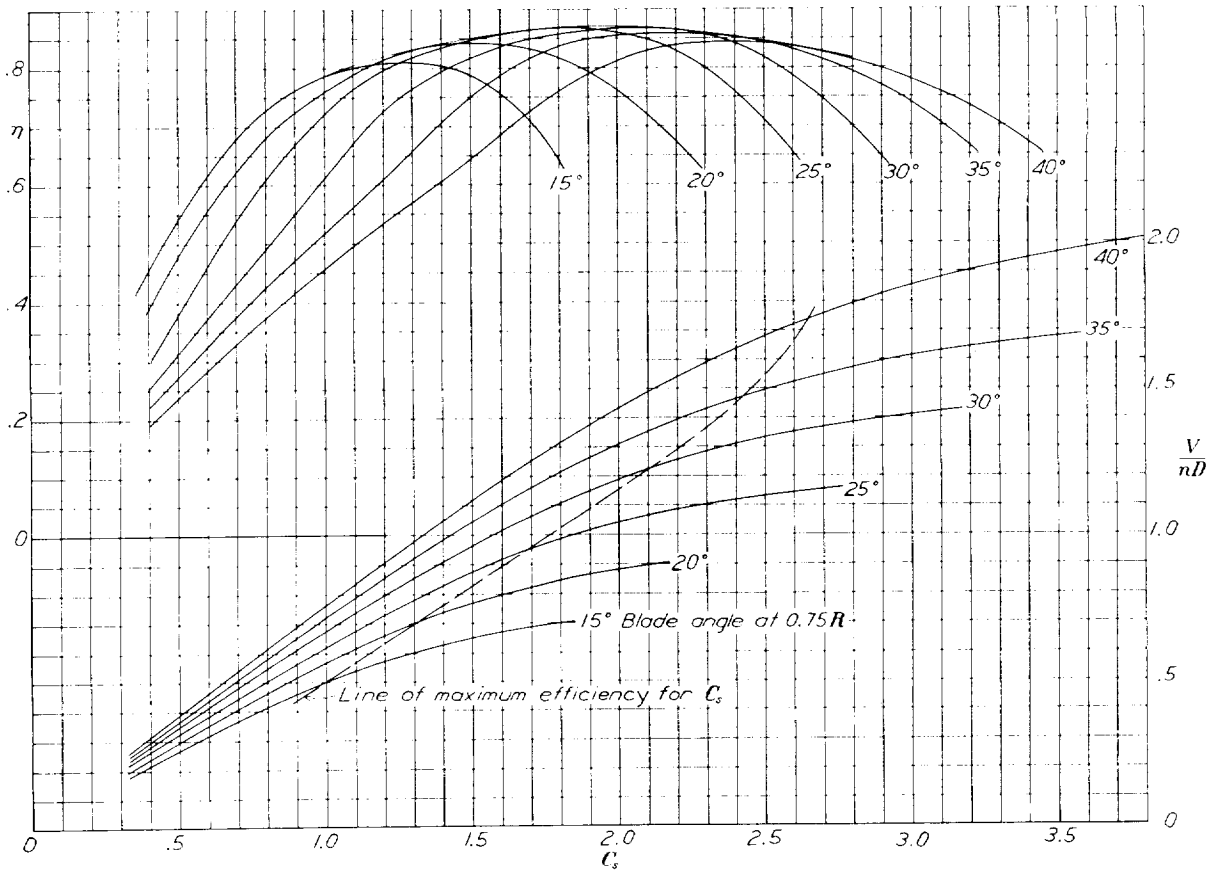

FIGURE 20. Design chart for propeller 6623-B (N. A. C. A. 4400 section inner half; N. A. C. A. 2400-34 section outer half).

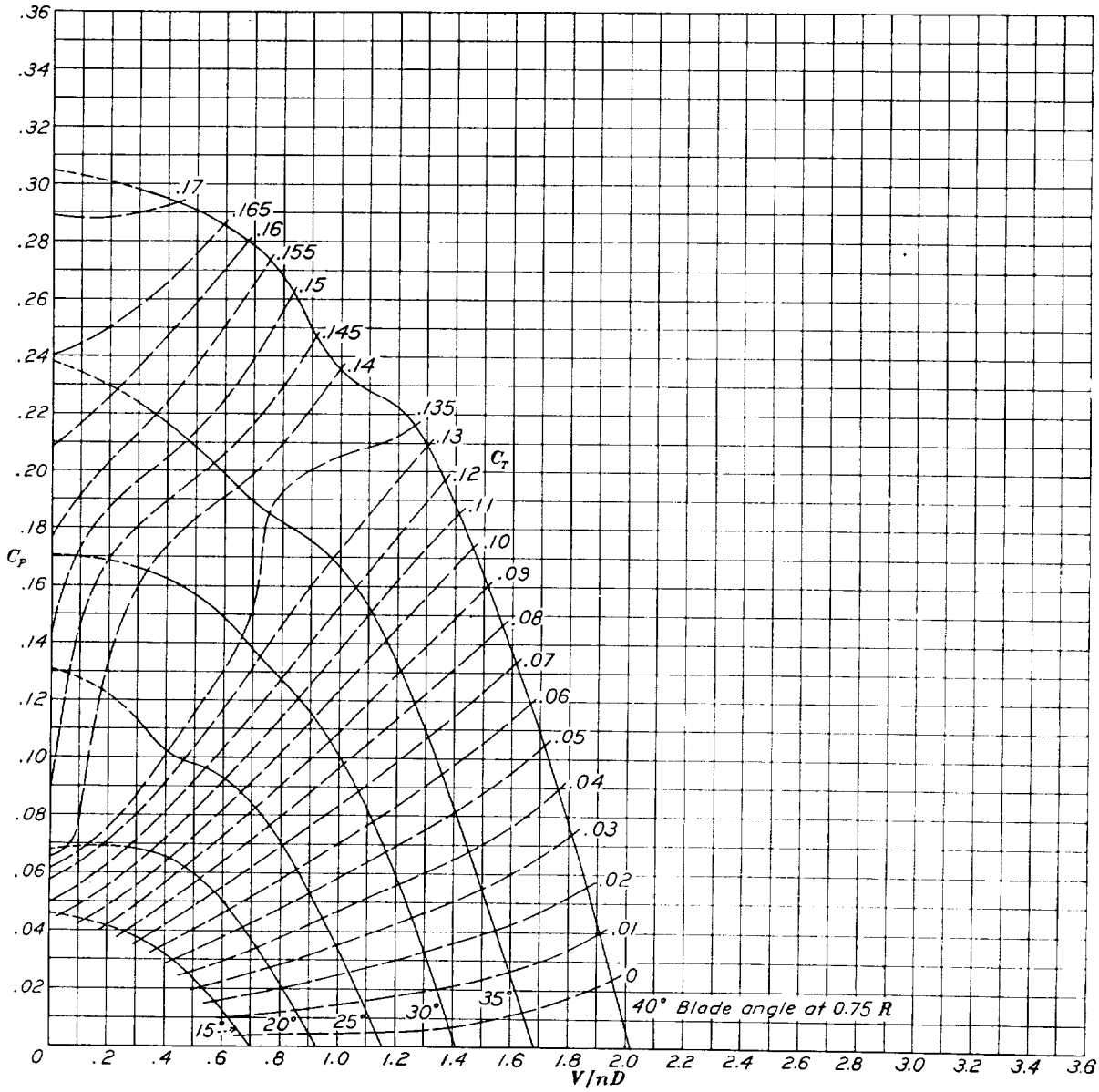

FIGURE 21.—Power-coefficient curves for propeller 6623-C (N. A. C. A. 2R200 section).

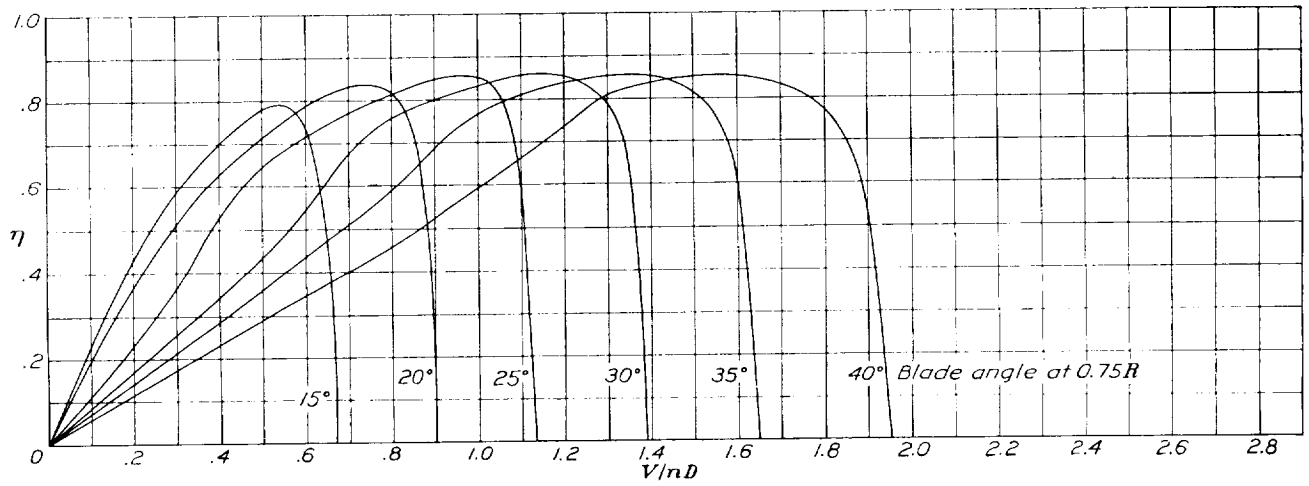

FIGURE 22.—Efficiency curves for propeller 6623–C (N. A. C. A. 2R$_3$00 section).

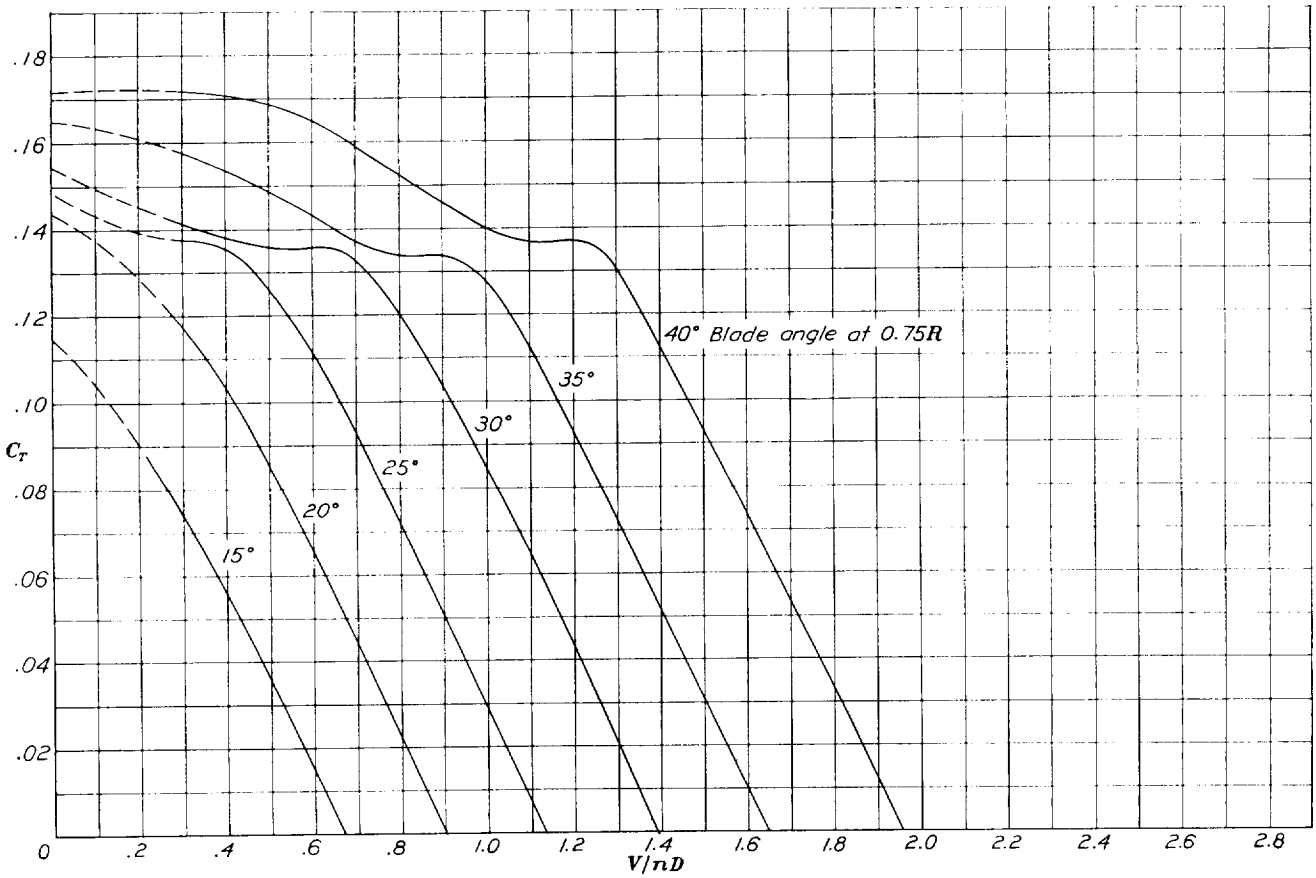

FIGURE 23.—Thrust-coefficient curves for propeller 6623–C (N. A. C. A. 2R$_3$00 section)

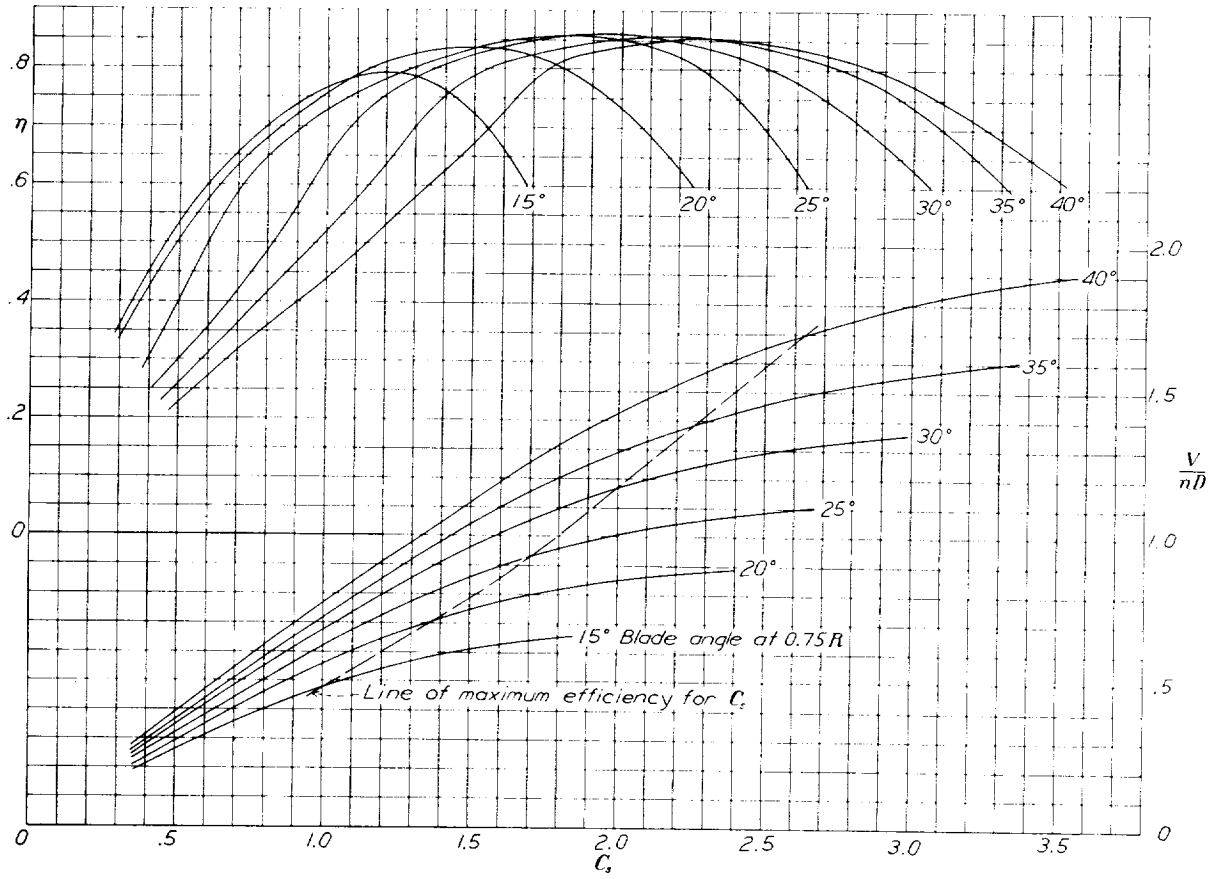

FIGURE 21.—Design chart for propeller 6623-C (N. A. C. A. 2R200 section).

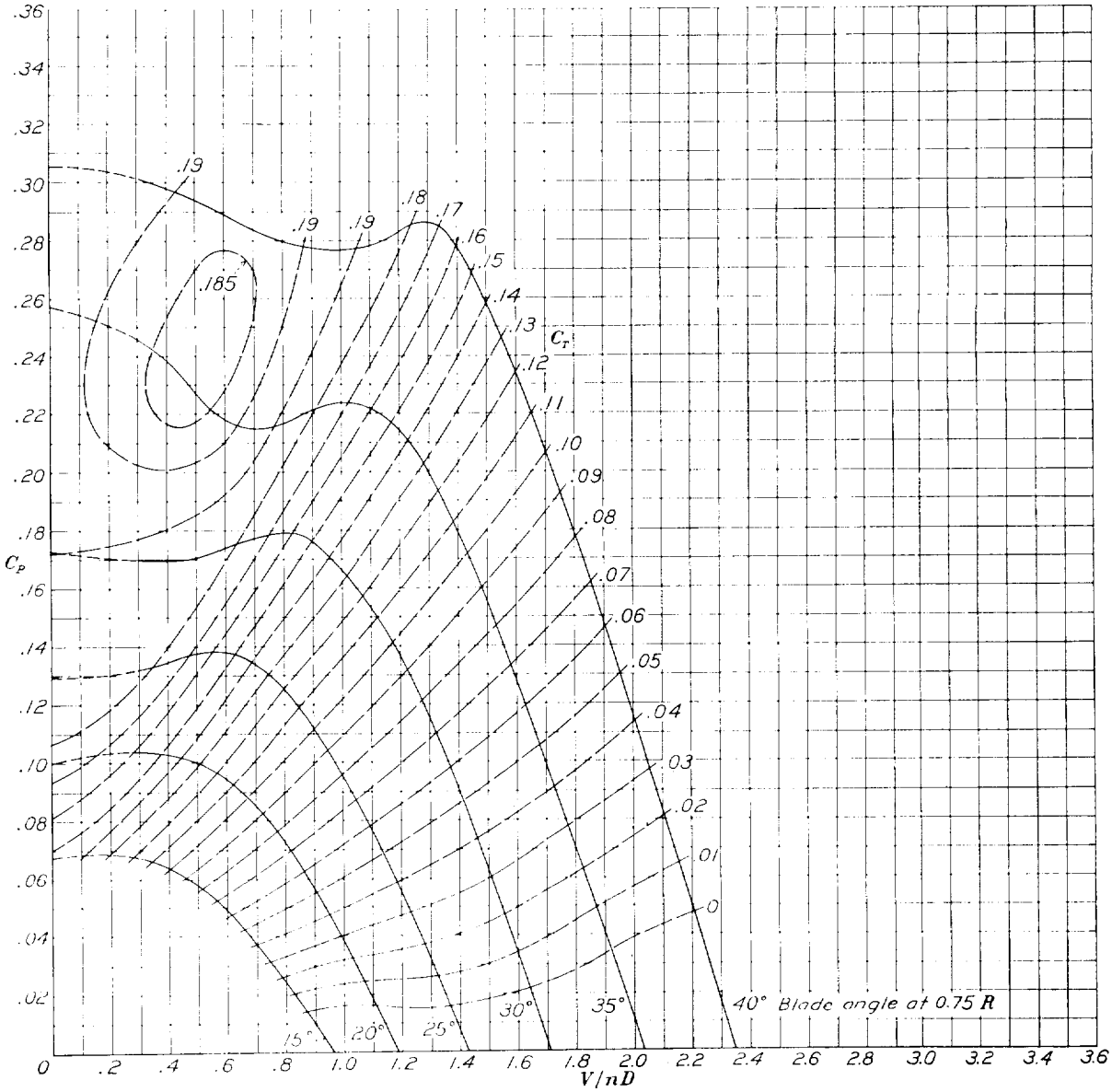

FIGURE 25.—Power-coefficient curves for propeller 6623-D (N. A. C. A. 6100 section).

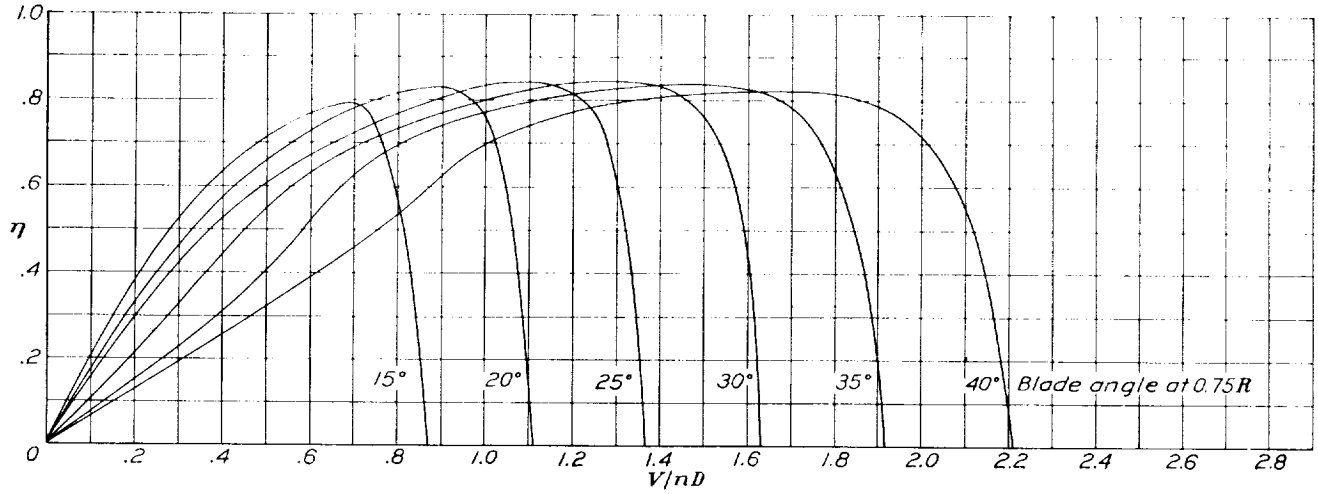

FIGURE 26.– Efficiency curves for propeller 6623-D (N. A. C. A. 6400 section).

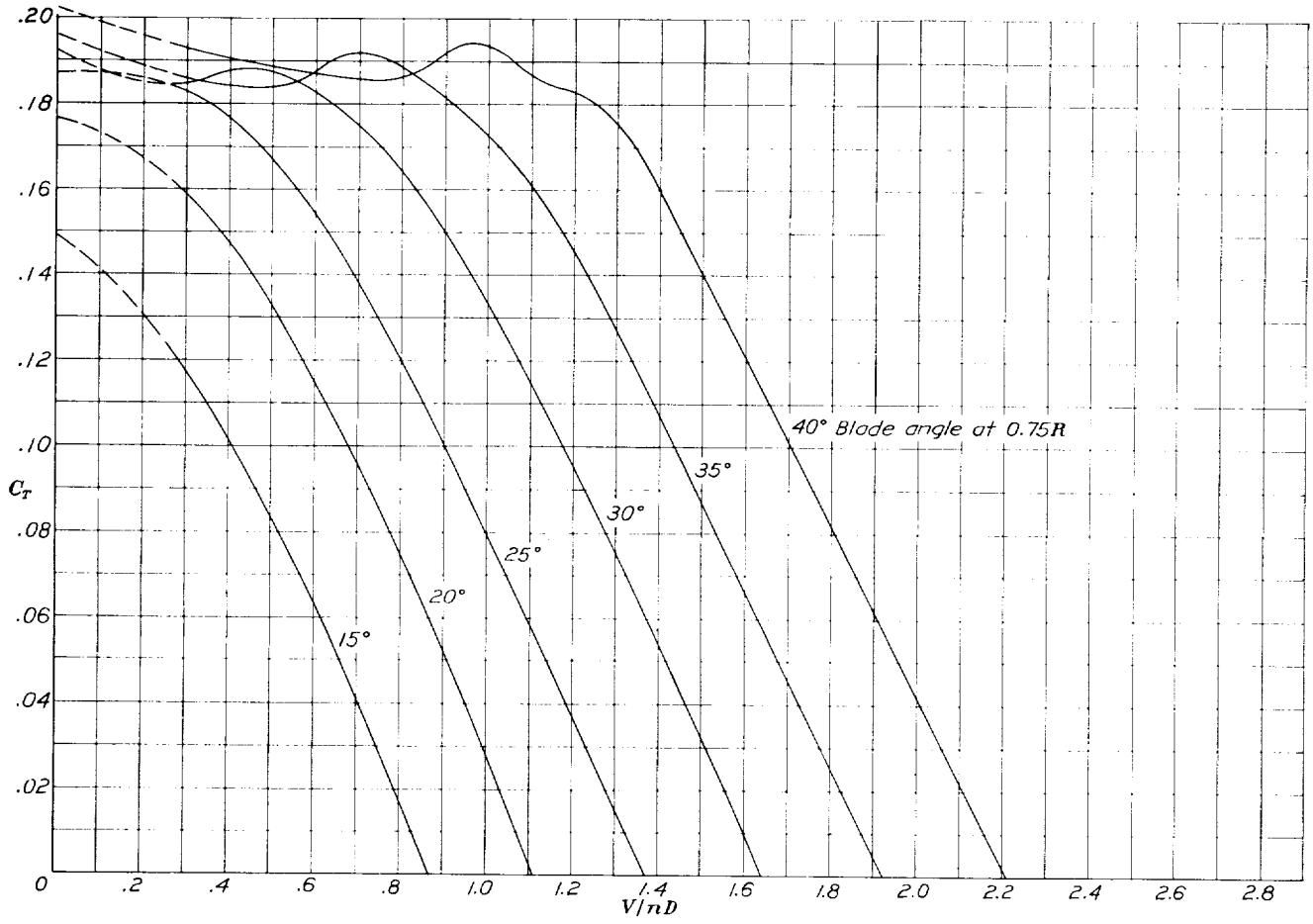

FIGURE 27.—Thrust-coefficient curves for propeller 6623-D (N. A. C. A. 6400 section).

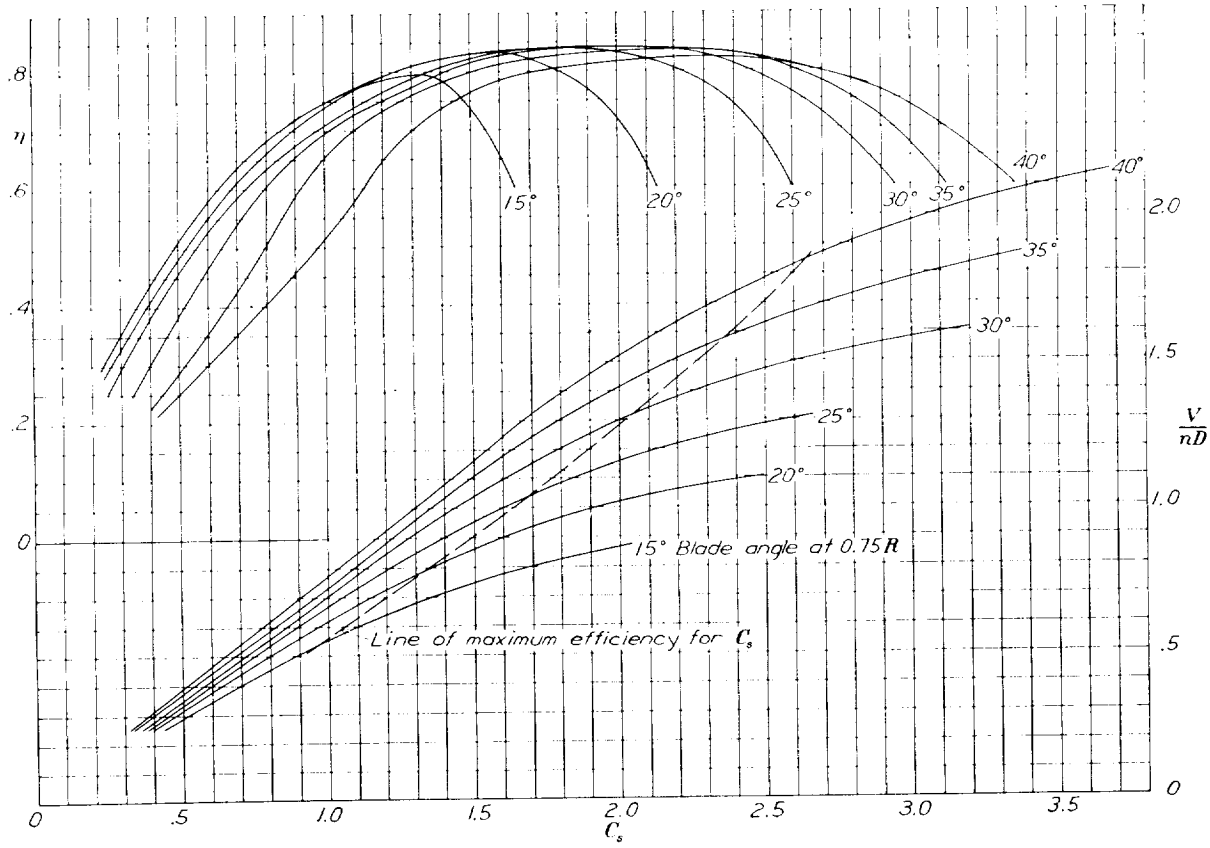

FIGURE 28. Design chart for propeller 6623–D (N. A. C. A. 6400 section).

DISCUSSION

Basic airfoil sections.—The thickness distribution and the camber lines for the six basic airfoil sections employed in the propeller designs are shown in figure 29. The thickness distribution (fig. 29 (a)) is about the same for all sections with two exceptions. The leading-edge radius of the N. A. C. A. 2400–34 section is shorter and the front portion is thinner than for the other sections; also, the point of maximum thickness occurs at 40-percent chord for the N. A. C. A. 2400–34 section and at 30-percent chord for the other sections. These thickness-distribution differences account for the superior qualities of this section at high speeds; because the radii of curvature of the upper surface are large,

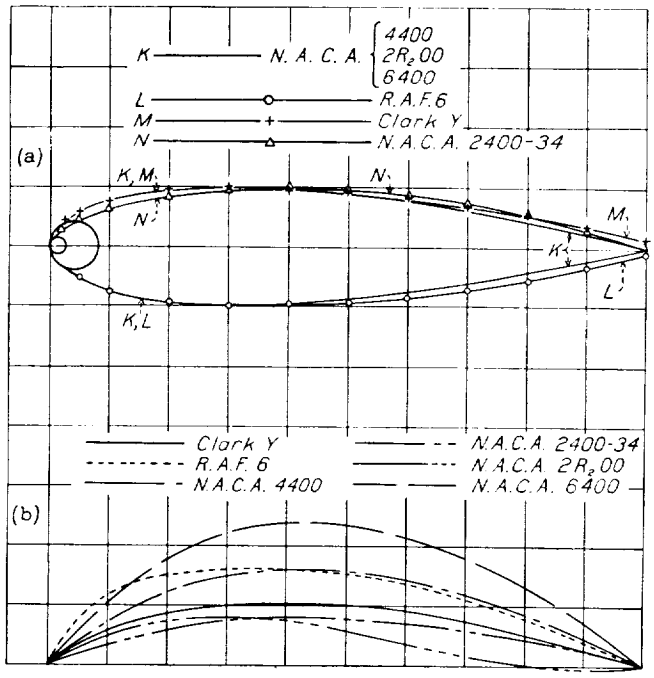

(a) Comparison of thickness-form curves.
(b) Comparison of camber lines for 0.75*R*.

FIGURE 29.—Comparison of thickness-form curves and camber lines. The chord lines for the R. A. F. 6 and the Clark Y sections have been shifted to bring the leading and trailing edges of the camber lines together.

the local induced velocities are kept small. Inasmuch as compressibility losses result from local velocities exceeding the velocity of sound, the critical speed for this section is delayed to higher values. The trailing-edge portions of the R. A. F. 6 and the Clark Y sections are slightly thicker than the others, but this difference in thickness distribution of the sections is probably of small importance.

Except for the thickness distribution of the N. A. C. A. 2400–34 section, the only essential physical differences between the sections are the shapes of the mean camber lines. The camber lines for the N. A. C. A. sections are mathematically derived curves and the camber ratios remain the same for all thickness ratios. In the design of the present propellers of N. A. C. A. section, the blade sections at different radii are thickened or thinned with respect to the basic section from the mean camber line, which remains constant. In contrast to this method, the Clark Y and the R. A. F. 6 sections are thickened or thinned from the chord line, which is also the lower surface. The mean camber lines are thereby different for each section thickness, the amount of camber being proportional to the thickness. In order to avoid differences in effective pitch distribution for all the propellers, the section blade angles were corrected for differences in the angles for zero lift.

The mean camber lines for the stations at 0.75 radius are plotted in figure 29 (b). Those for the R. A. F. 6 and the Clark Y sections have been plotted with respect to lines passing through the intersections of the camber lines and the leading and trailing edges and not with respect to the chord lines. The general shapes of the mean camber lines are similar for all of the sections except for the R. A. F. 6 and the $2R_200$ sections. The R. A. F. 6 section is characterized by the rapidly increasing camber at the nose of the section, and the camber line of the N. A. C. A. $2R_200$ section is reflexed.

The effect of the shape of the mean camber lines and the amount and position of maximum camber on the aerodynamic characteristics are fairly well established. In general, high cambers result in high values of $C_{L_{max}}$ and $C_{D_{min}}$ while low cambers result in low values of both $C_{L_{max}}$ and $C_{D_{min}}$. It is to be expected, therefore, that the maximum propeller efficiencies will reflect differences in the profile drag and that the efficiencies at low values of V/nD will reflect differences in maximum lift and in drag at high values of lift. In the selection of the sections, consideration was given to: the minimum drag, the maximum lift, the aerodynamic moment, and the speed at which the compressibility stall occurred. The N. A. C. A. $2R_200$, the N. A. C. A. 4400, and the N. A. C. A. 6400 sections constitute a series differing essentially in amount of camber and, consequently, display differences in $C_{D_{min}}$ and $C_{L_{max}}$. The N. A. C. A. $2R_200$ section was chosen in preference to the N. A. C. A. 2400 section for the 2-percent-camber group because it has a lower $C_{D_{min}}$ and it was thought that there might be some practical advantage in having a zero change in aerodynamic moment for controllable propellers. The N. A. C. A. 2400–34 section was selected because of its delayed compressibility stall.

Comparison of propeller characteristics.—In order to study the influence that the different sections exert on the propeller characteristics, superposed sets of curves of the thrust, the power, and the efficiency are given for three pitch-diameter ratios for zero thrust (figs. 30, 31, and 32). The pitch-diameter ratios of 0.82, 1.28, and 1.83 correspond to blade angles of 15°, 25°, and 35°, respectively, for the Clark Y propeller. The blade angles for the other propellers are slightly different, as may be noted.

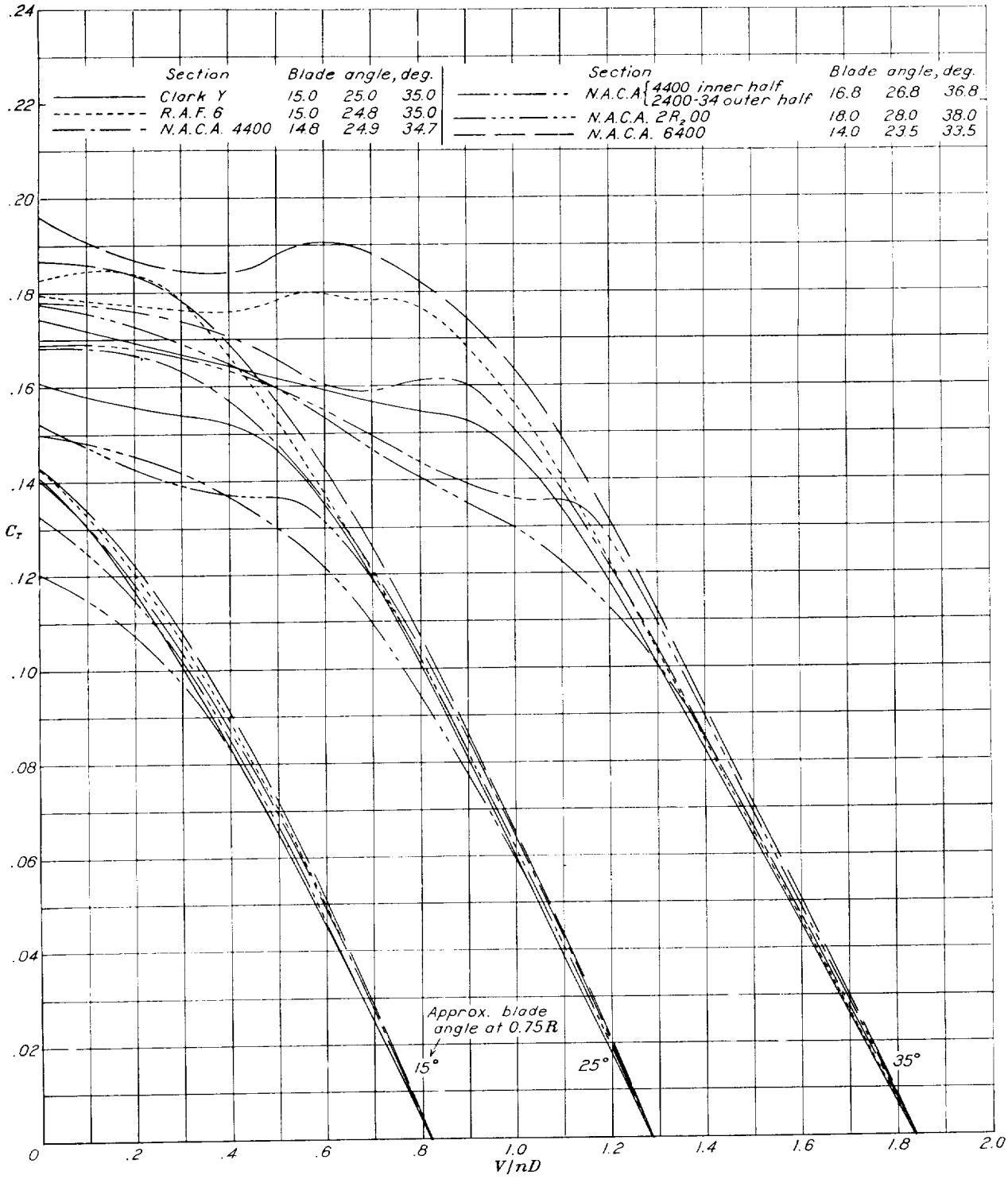

FIGURE 30.—Comparison of typical thrust curves.

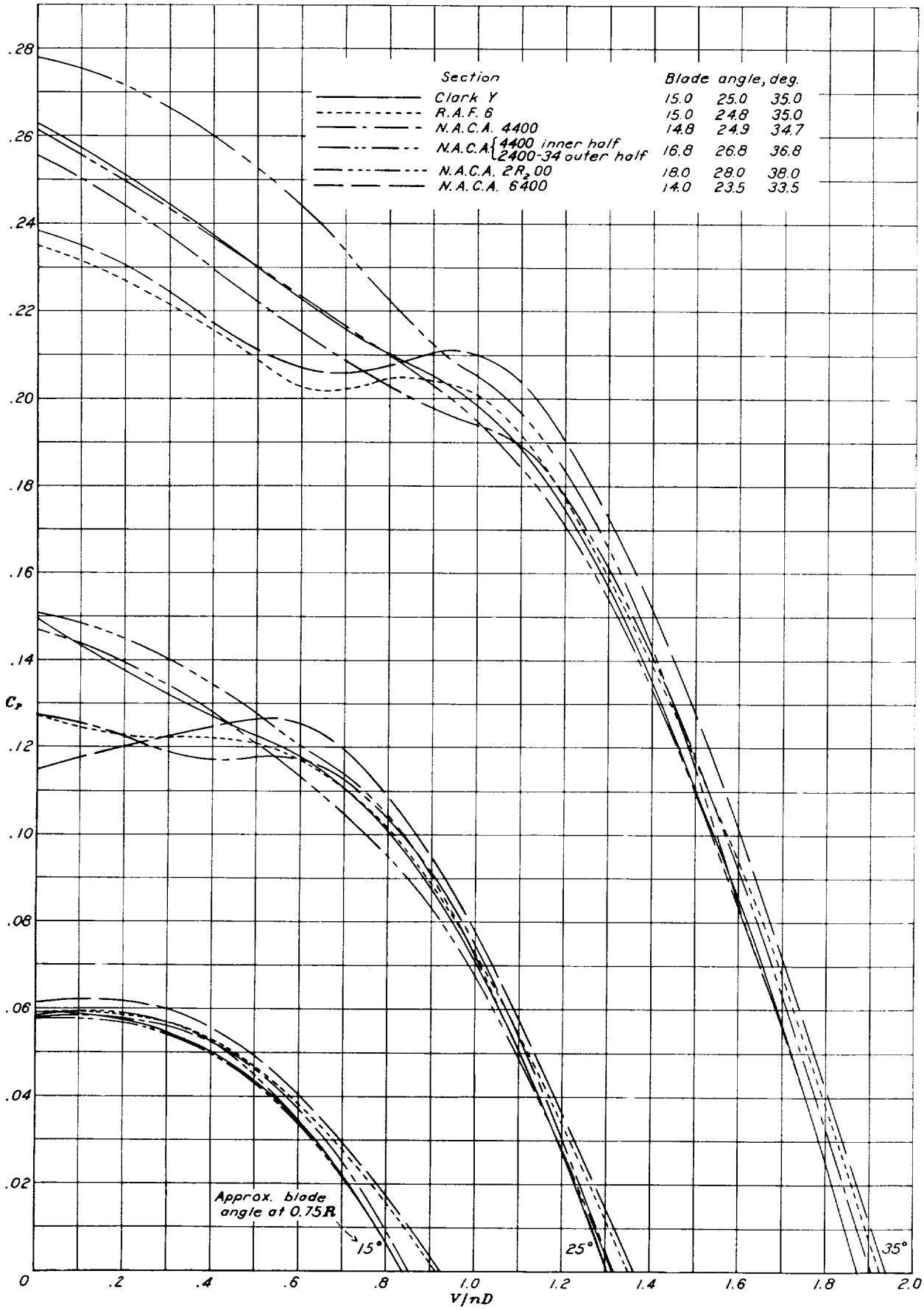

FIGURE 31.—Comparison of typical power curves.

The important difference in the thrust characteristics (fig. 30) attributed to the different sections is the value of C_T at which the blades stall. The propellers of 2-percent camber, the N. A. C. A. 2400–34 and the N. A. C. A. 2R200 sections, stall at a C_T value of about 0.13; the propeller of 4-percent camber, the N. A. C. A. 4400 section, stalls at about 0.15; and the propeller of 6-percent camber, the N. A. C. A. 6400 section, at about 0.19. The curves indicate that the propeller of Clark Y section has an average camber ratio of about 0.035 for the entire propeller, inasmuch as the stall is at a C_T value of about 0.15. The average camber ratio is higher than that for the 0.75 radius station (0.026), probably owing to the fact that the inboard sections are all definitely more highly cambered while the outboard ones are only slightly less cambered. The propeller of R. A. F. 6 section has a higher average effective mean camber ratio than that of its 0.75 radius station for the same reason; it is 0.055 as compared with 0.040.

The corresponding power curves are given in figure 31. In the region where all the propellers are stalled, it may be seen that the high-camber propellers have lower power coefficients than the low-camber ones.

The efficiency curves, given in figure 32, indicate the effect of profile drag on maximum efficiency. The propellers of low camber display efficiencies about 3 percent higher than for the ones of high camber, and the peaks occur at higher values of V/nD. Both effects are attributed to the lower profile drags of the low-camber propellers. The lower the profile drag, the closer the efficiency approaches the ideal for which the profile drag is zero. Also, the ideal efficiency is highest at zero thrust, which explains why the peak efficiencies occur at higher values of V/nD for the low-camber propellers. This shifting of the peaks to higher values of V/nD for propellers of decreasing profile drag is of importance in design work. The closer the V/nD for peak efficiency approaches the V/nD for zero thrust, the smaller is the power coefficient and, consequently, the greater the diameter. The extreme condition is for a propeller with the ideal efficiency, i. e., maximum efficiency occurring at zero thrust and zero torque so that the diameter is infinite and the rotational speed zero. The significance of the diameter will be clarified by computations later in the report.

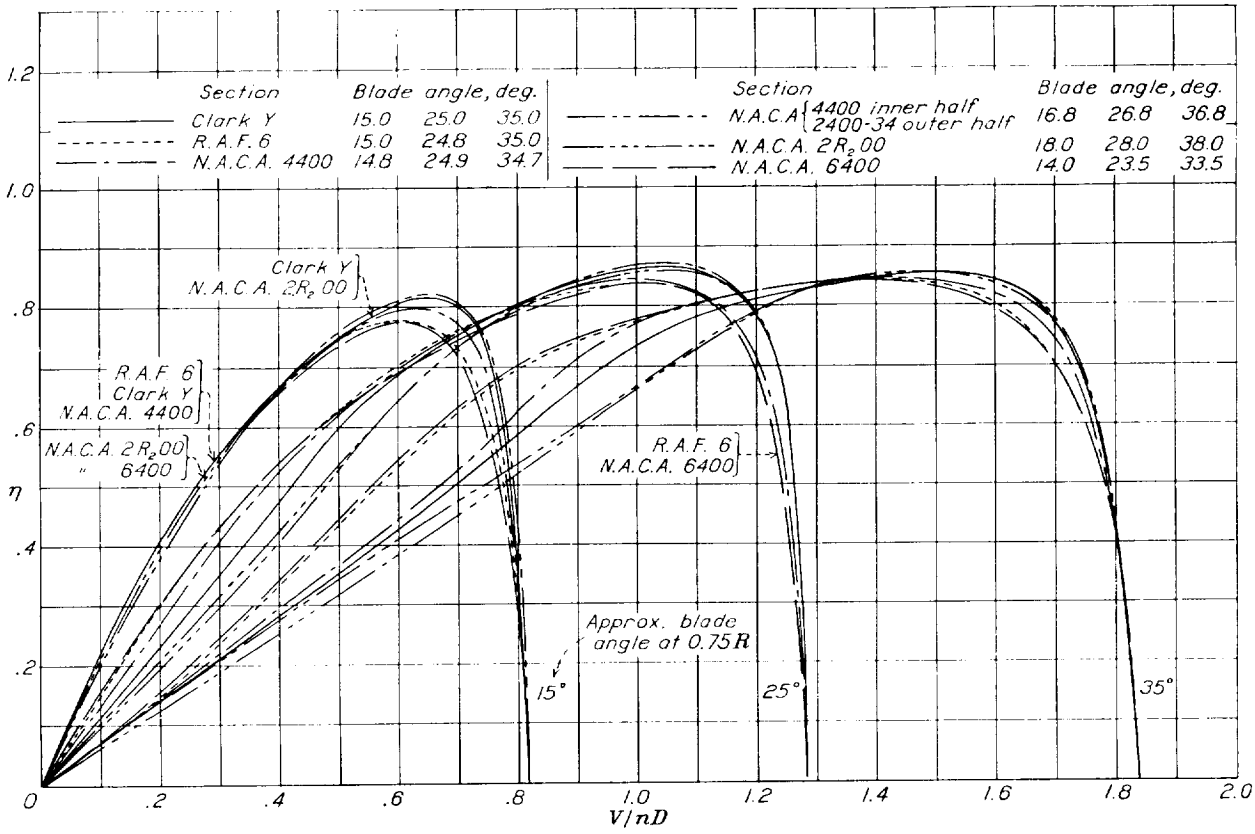

FIGURE 32.—Comparison of typical efficiency curves.

The efficiency curves also reflect the high-thrust and the low-drag values observed for the high-camber propellers operating at low values of V/nD. These differences in efficiency, however, do not necessarily represent true differences in thrust power available for either fixed-pitch or controllable propellers. In the case of a combination of a fixed-pitch propeller and an engine, differences in C_{P_0} (design power coefficient) will determine differences in diameter, so that for a given take-off speed there will be differences in V/nD, η, and also engine speed, N. The thrust horsepower available, if constant torque is assumed, is obtained from

$$\text{t. hp.} = (\text{b. hp.})_0 \frac{N}{N} \eta$$

where N_0 is the engine speed at the high-speed condition

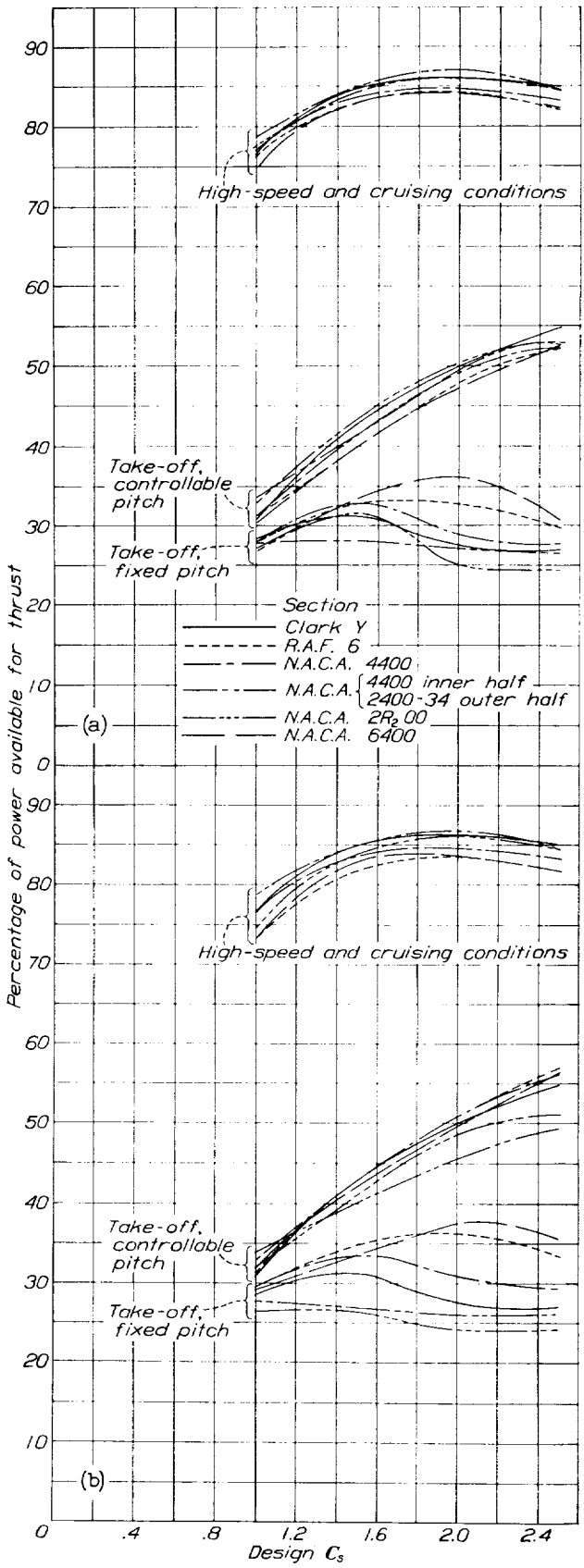

(a) All propellers designed for maximum efficiency at high speed.
(b) All propellers have same diameter for a given C_s (Clark Y propeller used as standard).

FIGURE 33.—A comparison of propellers for the high-speed and take-off flight condition. Take-off criterion, $V=0.25V_{max}$.

of flight. In the case of controllable propellers, the pitch is adjusted to maintain C_{P_0} and N_0 constant so that different propellers will be set at different blade angles for the same V/nD or air speed. In order to show the effect of the different blade sections on performance, the thrust power available is computed and will be discussed later for both fixed-pitch and controllable propellers.

Effect of blade section on the performance of engine-propeller combinations.—Any conclusion drawn from comparisons of relative engine-propeller performance depends somewhat on the methods employed in the analysis. If each propeller is selected for maximum efficiency at high speed, the diameters of the various propellers will be different, depending upon the design power coefficient, C_{P_0}, which in turn depends on the V/nD for peak efficiency. The differences in diameters will have a large effect on the efficiency at the take-off condition; for controllable propellers the larger the diameter, the higher the efficiency. If the V/nD for peak efficiency could be determined with uniform accuracy for all propellers, the comparison would be a just evaluation of the relative merits, compressibility or tip-speed effects due to the differences in diameters being neglected.

If the propellers are compared on a basis of equal diameters for a given design condition, all the propellers will not operate quite at peak efficiency at high speed. The high-camber propellers will operate beyond the peak and the designs will be, in effect, "compromises" because the take-off efficiencies for controllable propellers, at least, will be increased thereby. The constant-diameter method has the advantage of comparison at equal tip speeds, and the airplane structural limitations on the diameter are often the determining factor.

As neither method is entirely satisfactory and both have their merits, computations have been given for each. In some instances the results appear to be contradictory but, if the methods are well understood, a reasonable interpretation can be made.

In figure 33 (a) the propellers are compared on the basis of maximum efficiency for high speed. Curves are given for high-speed efficiency, for take-off efficiency for controllable propellers of the constant-speed type, and for take-off efficiencies for fixed-pitch propellers, all for a wide range of design conditions (values of design C_s from 1.0 to 2.5). The take-off criterion is assumed to be the thrust power available at a speed equal to 0.25 of the high speed of landplanes. This value corresponds to 0.7 of the take-off speed for airplanes having a speed ratio of high speed to take-off speed of 2.8. It can be shown that 0.7 of the take-off speed is the best single point for comparing take-off thrust as that point represents the approximate center of the area of the graphically integrated diagram of take-off run of most airplanes represented by $\int t dv$, where t and v represent time and velocity, respectively.

In the computation of the take-off thrust power, the engine torque is assumed to be equal to the torque at high speed. The engine speeds are assumed to remain constant for the controllable propellers but to decrease for the fixed-pitch propellers in the take-off condition, according to the relation

$$\frac{N}{N_0}=\sqrt{C_{P_0}/C_P}$$

Although the percentage of thrust power available also represents propulsive efficiency for the controllable propellers, it represents $\eta(N/N_0)$ for the fixed-pitch propellers.

The greatest difference in maximum efficiency is about 3 percent; the highest efficiencies are for the low-camber propellers.

It seems strange that the controllable propellers of low and medium camber would also excel for the take-off condition. This paradox is explained by the results presented in table IV. The low-camber propellers are designed with larger diameters than the high-camber ones and, in order to absorb the same power at the take-off, are set to lower blade angles for which the efficiency is higher.

The high-camber propellers are definitely superior for fixed-pitch propellers set at high blade angles. The reason is quite obvious. (See figs. 30, 31, and 32.) The stall is delayed to higher angles of attack, i. e., to lower values of V/nD, and the gain in efficiency due to the lower drag and the higher lift of the sections is quite pronounced. The decrease in engine speed also plays a prominent part in the available thrust power, as is shown in table IV. The high-camber propellers are designed to operate at higher values of C_{P_0} than the low-camber ones. The higher the C_{P_0}, the less is the increase in C_P for take-off and, consequently, the less is the drop in rotational speed. The stalling characteristics of the propellers do not enter the problem for low blade angles so that there is less choice of section for low design C_s conditions.

In figure 33 (b) the propellers are compared on a basis of equal diameters for given values of C_s. The propeller of Clark Y section is taken as the standard because it is of medium camber. The diameters of the low-camber propellers are slightly decreased from the previous comparison and those for the high-camber ones are increased. The high-speed efficiences are slightly different from the maximum values but the order of merit is the same.

The order of take-off efficiencies for the controllable propellers is changed. The high-camber propellers are about equal, in general, to the medium-camber ones, and the low-camber ones have the lowest efficiencies. The medium-camber and the high-camber propellers are about equal in this comparison because neither type exceeds the stall for the take-off criterion (see table V); the superior stalling characteristics of the high-camber propellers are, of course, not utilized. The high-camber propeller is slightly superior at a C_s value of 2.5, which shows that its stalling characteristics are beginning to be utilized and, for higher C_s values, they should be definitely superior. The high-camber propellers would have been superior at lower values of C_s if the diameters had all been smaller. For example, if the propeller of R. A. F. 6 section had been assumed to be the standard of comparison instead of the propeller of Clark Y section, the high-camber propellers would have excelled at C_s values above 1.5.

Large differences in take-off thrust power are evident for the various fixed-pitch propellers. This comparison is the closest representation given of a pure efficiency comparison because the take-off C_P has about the same value for all propellers; they therefore all have about the same drop in engine speed. The results given in figure 32 show the same order of merit in the take-off

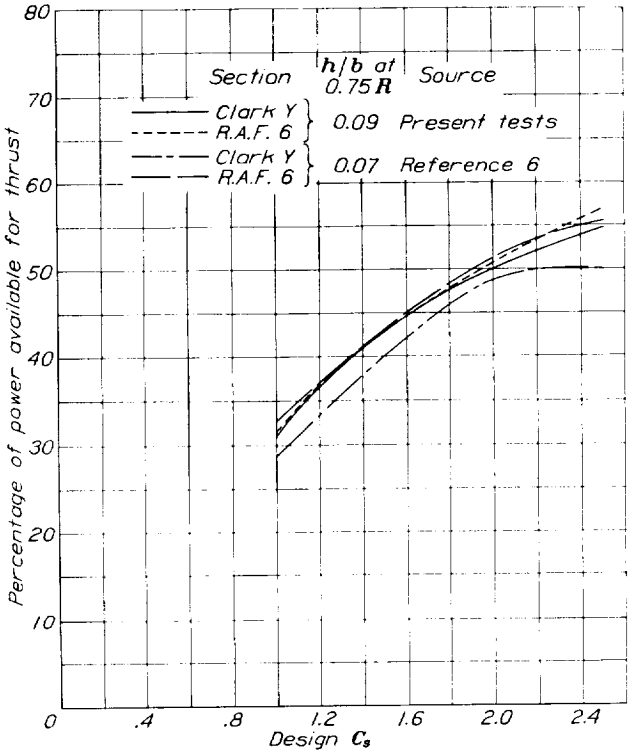

FIGURE 31.- Comparison of propellers of Clark Y and R. A. F. 6 section of two thickness ratios for the take-off condition. $V=0.25V_{max}$, controllable operation; all propellers have the same diameter.

range as the comparison in figure 33 (b); both methods indicate the superiority of high-camber propellers for medium and high blade-angle design conditions.

Effect of thickness.—In reference 6, comparisons were made between propellers of three different sections: Clark Y, R. A. F. 6, and N. A. C. A. 2400-34. The propellers were thinner than the present ones ($h/b=0.07$ at $0.75R$ as compared with $h/b=0.09$). In the former comparison, based on controllable propellers of equal diameter, the propeller of R. A. F. 6 section was best for take-off, while the present tests indicate the propellers of Clark Y and R. A. F. 6 sections to be about

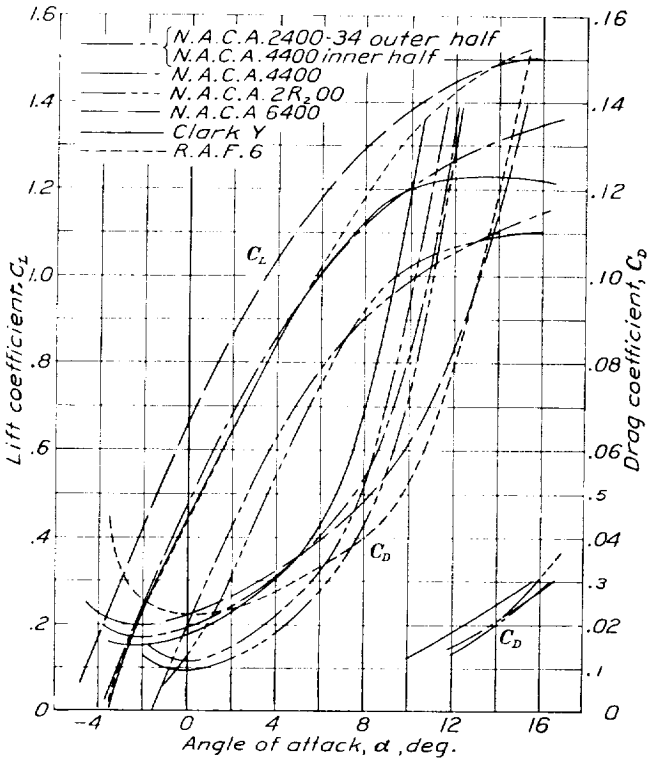

FIGURE 35.— Airfoil characteristics of propeller sections computed from the 0.70R station. Blade angle, 25° at 0.75R.

equal. It is reasonable to assume that the differences in relative efficiency are due to the differences in thickness of the two sets of propellers. Figure 34 shows that the propeller of Clark Y section improves in take-off efficiency with increasing thickness whereas the propeller of R. A. F. 6 section does not. It is well known that $C_{L_{max}}$ increases with airfoil thickness and camber up to a limit. As the R. A. F. 6 section has a higher camber than the Clark Y, it seems logical that it would reach its $C_{L_{max}}$ limit at lower values of thickness. Reference 2, which is a more general study of the effect of blade thickness, seems to substantiate this contention.

The N. A. C. A. section propellers are not so sensitive to change in thickness because the camber is not a function of thickness.

Lift and drag coefficients reduced from propeller results.—In reference 7, Lock presents two methods of reducing propeller characteristics to airfoil results and vice versa. In one method, computations are made for six blade elements and the thrust and the torque grading curves are integrated. The second method is based on only a single radius, the assumption being that the shape of the grading curves remains constant so that a constant integrating factor is used. This method is further simplified by the use of charts so that a propeller may be analyzed within an hour.

Lift and drag curves derived by the single-radius method are plotted against angle of attack in figure 35 for the six propellers with a blade-angle setting of 25° at 0.75R; polar curves are given in figure 36. The results for only one blade angle are analyzed. The tests from which these curves are derived were made the same day under apparently identical conditions and are therefore considered to be relatively more accurate than for the whole series; the estimated precision is within 0.5 percent for η_{max}.

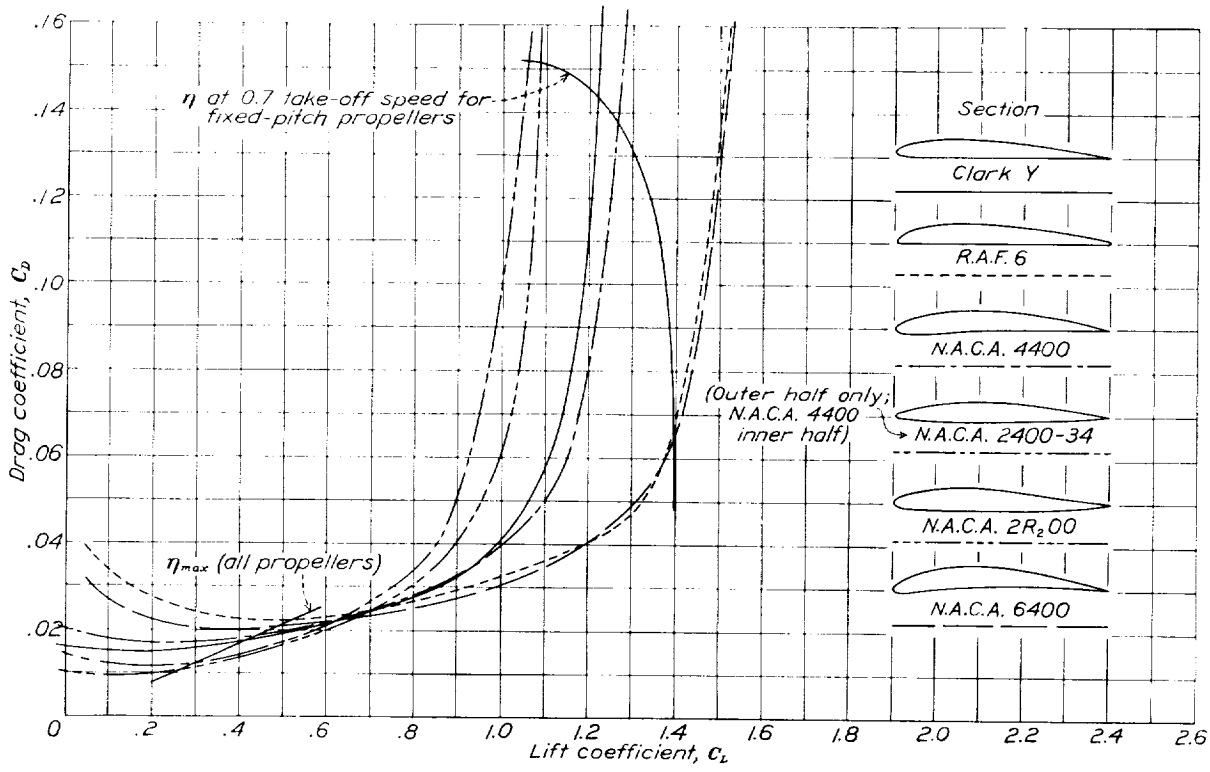

FIGURE 36.— Polar airfoil section characteristics reduced from propeller results. V/V_t=0.46 (approximately); blade angle, 25° at 0.75R.

Of interest are $C_{D_{min}}$, $C_{L_{max}}$, and C_D at high values of C_L. The sections of 2-percent camber show values of $C_{D_{min}}$ of about 0.01; the sections of 4-percent camber show values of about 0.017; and the section of 6-percent camber shows a value of about 0.02. The propeller of R. A. F. 6 section, which has a camber line (see fig. 29) different from the other sections, shows the highest $C_{D_{min}}$, 0.022. The 2-percent sections show values of $C_{L_{max}}$ of about 1.1; the 4-percent section, of about 1.3; and the 6-percent section, of about 1.5.

Lift and drag coefficients are of little value in determining the relative merits of the airfoil sections for propellers unless their quantitative importance is determined. The influence of C_D at η_{max} (approximately $C_{D_{min}}$) on η_{max} is given in figure 37 for the propellers when set at a blade angle of 25° at $0.75R$. Large changes in C_D are seen to affect η_{max} only a small amount. Reducing C_D from 0.02 to 0.01 increases η_{max} only 3 percent. By extrapolation, if the drag could be reduced to zero, the η_{max} would be increased only to

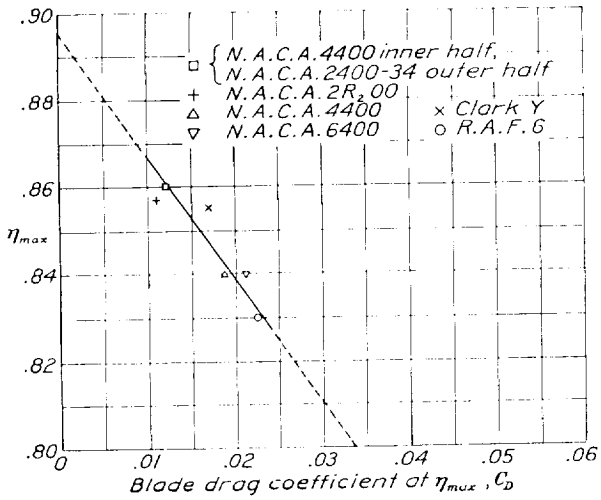

FIGURE 37.—The influence of the blade drag coefficient on the maximum propulsive efficiency. Blade angle, 25° at $0.75R$.

0.895, which is only a few percent below the ideal for this condition. (The ideal efficiency neglects profile drag, hub drag, body slipstream drag, rotational losses, tip losses, blade interference, etc.) This result indicates that the possibilities for improving η_{max} by reducing the profile drag of the sections are very limited; the maximum increase is probably not more than 1 or 2 percent above that for the present-day standard sections. It should be emphasized that figure 37 applies only to a blade-angle setting of 25°. For higher angles up to about 45°, according to the simple blade-element theory, C_D would have a slightly smaller influence on η_{max}.

A direct relationship does not always exist between $C_{L_{max}}$ and take-off efficiency because in many cases the stall is not reached. Fixed-pitch propellers set at blade angles below about 20° (the approximate blade angle for stalling at zero air speed) and some controllable propellers set at angles as high as 30° do not stall during the take-off run. Probably some indirect relationship exists, however, between $C_{L_{max}}$ and the take-off efficiency because of the drag at high angles of attack associated with sections of different camber.

The relationship between the $C_{L_{max}}$ and the take-off efficiencies of controllable and fixed-pitch engine-propeller combinations is given in figure 38. In figure 38 (a) the analysis is based on propellers designed for η_{max}, the data being taken from figures 33 (a) and 35.

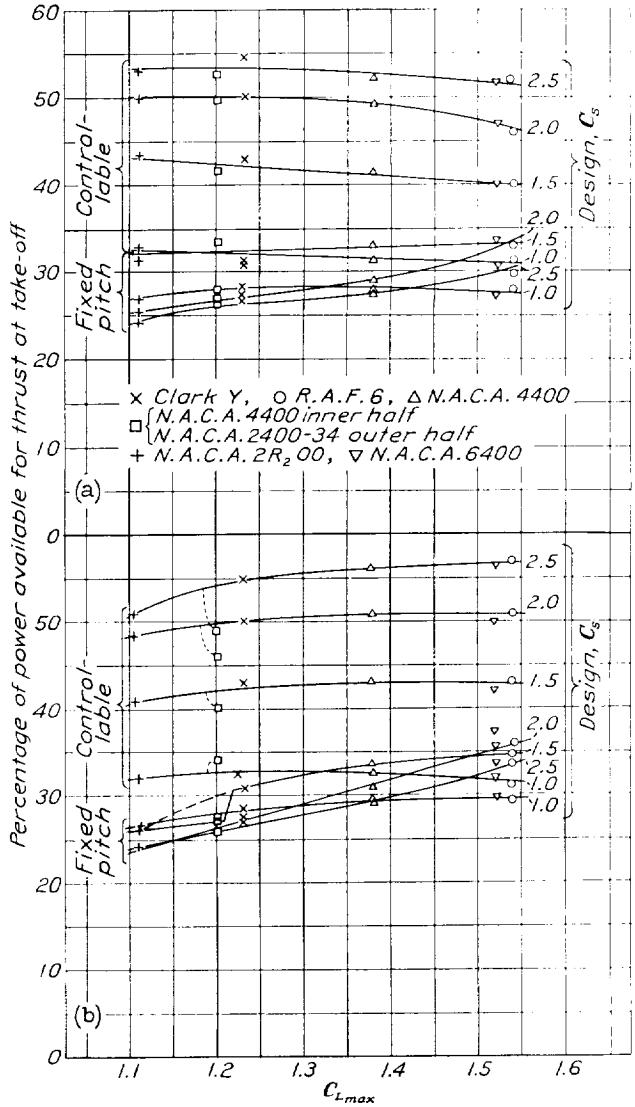

(a) All propellers designed for maximum efficiency at high speed.
(b) All propellers have same diameter for a given C_s (Clark Y propeller used as standard).

FIGURE 38.—Relationship between $C_{L_{max}}$ and the propeller characteristics for the take-off condition. Take-off criterion, $V=0.25V_{max}$.

It may be seen that increasing values of $C_{L_{max}}$ are associated with a slightly decreasing take-off thrust power of controllable propellers. This trend, as previously explained, is due to the different take-off blade settings necessitated by the differences in diameter.

The trend of take-off thrust power increases with increasing $C_{L_{max}}$ for the fixed-pitch propellers set at moderately high blade angles but not for the low blade-angle settings because the blades are never stalled.

In figure 38 (b) a similar analysis is presented for propellers having equal diameters, the material being taken from figures 33 (b) and 35. In this example, increasing values of $C_{L_{max}}$ are associated with an increasing take-off thrust power of controllable propellers for only the low C_L range and the high design C_s values. The high-pitch low-camber propellers are the only ones exceeding the stall at the take-off, as previously pointed out. Had the diameters of all propellers been smaller, more propellers would have exceeded the stall and the advantage of a high lift coefficient would be more general.

The advantage of high lift coefficients for fixed-pitch propellers is definite over the entire range investigated; it is more definite, however, for the high blade angles than for the low ones. The take-off thrust is increased an average of 1 percent for each 1 percent increase in $C_{L_{max}}$ for C_s values of 1.5 and over.

Effect of compressibility.—In the tests reported in reference 8 it was noted that propellers of R. A. F. 6 section were more affected by compressibility in the take-off and climbing range than those of Clark Y section. It is reasonable to assume that the other propellers would likewise display differences. Of the sections incorporated in the present propellers, the Clark Y, the R. A. F. 6, and the N. A. C. A. 2409-34 have been tested as airfoils in the N. A. C. A. high-speed wind tunnel and the results are given in figure 39 (from references 1 and 4). The low-speed results, $V/V_c=0.40$, correspond approximately to the present results. It may be noted that the curves from these tests of low-speed airfoils check in a relative way the airfoil curves derived from the propeller results.

In the airfoil curves for high speed ($V/V_c=0.80$, fig. 39), it may be noted that the values of the minimum drag coefficient of the N. A. C. A. 2409-34 section was doubled, the Clark Y tripled, and the R. A. F. 6 nearly tripled by doubling the air speed. If all the elements were traveling at $0.80V_c$, the maximum efficiency of the propeller of N. A. C. A. 2400 34 section would be expected to drop about 3 percent, that of Clark Y section about 9 percent, and that of R. A. F. 6 section about 8 percent, judging by the effect of drag on η_{max}, as shown in figure 37 for the 25° blade-angle setting. Fortunately, only the tip elements are affected so the loss is much less.

For the 2-blade propeller of R. A. F. 6 section turning at 1,800 r. p. m. ($V/V_c=0.83$), the loss in peak efficiency is only about 1 percent (within the experimental error) (fig. 40), which means that very little area at the tips is affected. These results have been translated into airfoil results and are shown in figure 41 for the purpose of comparison with the high-speed results shown in figure 39. Some idea of the blade

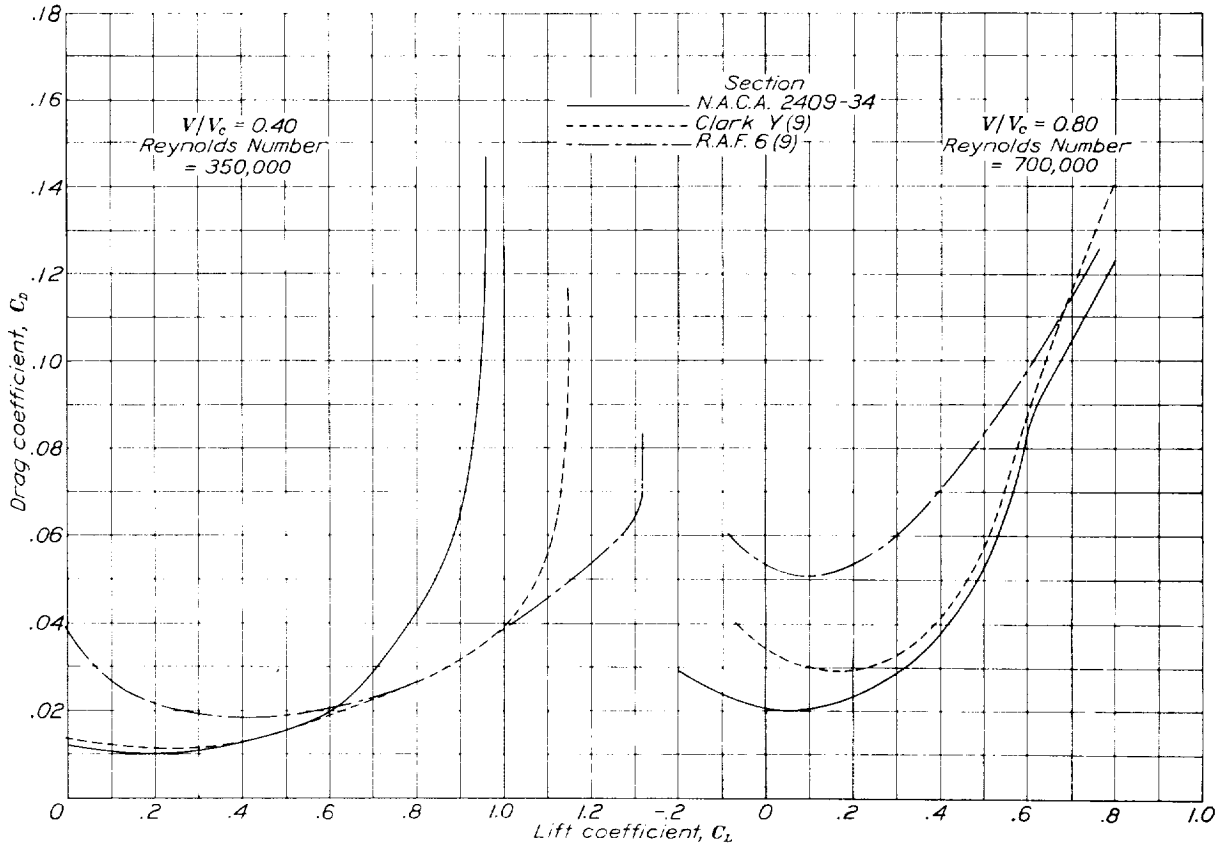

FIGURE 39.—Characteristics of three airfoils at two air speeds as measured in the N. A. C. A. 11-inch high-speed tunnel (from references 1 and 4).

area affected may be obtained by referring to figure 42 wherein C_D is plotted against V/V_c (which is also a function of propeller radius, assuming only rotational velocity). If consideration is given to the

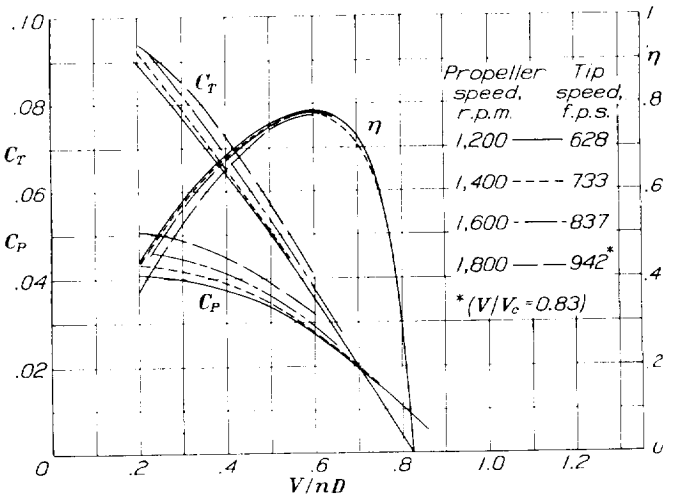

FIGURE 40. Effect of compressibility on the characteristics of an R. A. F. 6 propeller (from reference 8).

thrust distribution over the blade, which falls off near the tip, it is readily seen why the propeller of the R. A. F. 6 section loses so little in peak efficiency owing to compressibility.

It is pointed out in reference 4 that the N. A. C. A. 2400–34 series section is superior at high speeds to the

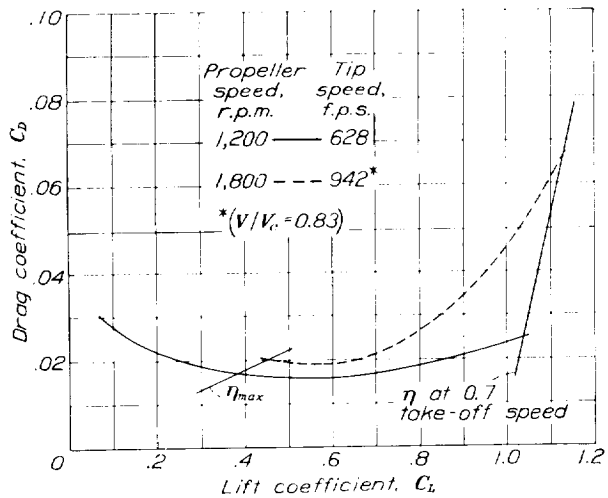

FIGURE 41.- Airfoil section characteristics reduced from propeller results. Two-blade propeller of R. A. F. 6 section; blade angle, 15° at $0.75R$ (from reference 8).

commonly used propeller sections and the curves that are herein reproduced in figure 39 are given as evidence. As a result of the recommendations of reference 4, propeller 6623-B was designed with the N. A. C. A. 2400–34 series section for the outer half. This propeller was not tested at high tip speeds because the propeller of R. A. F. 6 section showed scarcely any decrease in peak efficiency; it was concluded that any compressibility effects of the propeller of N. A. C. A. 2400-34 section could not be measured at η_{max} with the present test set-up.

Figure 42 shows the relative blade area affected by compressibility for the propellers of R. A. F. 6 and N. A. C. A. 2400-34 sections. It appears that the tip speed must be at least $0.90V_c$ before compressibility effects at η_{max} could be measured on the propeller of N. A. C. A. 2400–34 section, and then the loss would probably amount to not more than 1 percent, judging by the results for the R. A. F. 6 section for a tip speed of $0.83V_c$. The results of reference 9 also show that no loss in peak efficiency occurs up to

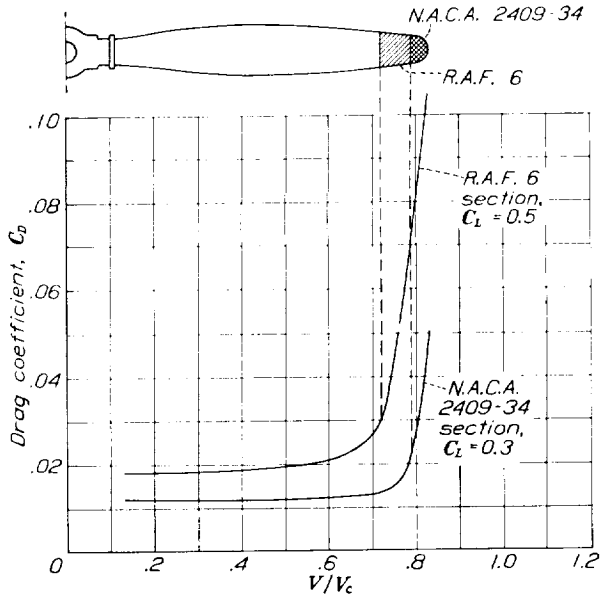

FIGURE 42.—Effect of compressibility on the drag of two sections when working at lift coefficients for maximum propeller efficiency (from reference 4). Blade area appreciably affected by compressibility for a tip speed equal to $0.83V_c$.

tip speeds of 0.85 or $0.90V_c$ for the standard propeller sections.

Tests of the propellers with the N. A. C. A. sections at high tip speeds for the take-off and climbing conditions are planned. It is not anticipated, however, that the condition of high tip speed will materially alter the relative merits of the sections for the take-off condition because: First, only the tip sections ordinarily operate at high speeds; and, second, compressibility tends to equalize the characteristics of different airfoils at high angles of attack rather than to accentuate any differences. Figure 39 indicates that all airfoil sections have about the same $C_{L_{max}}$ at $0.80V_c$. This result was also found to be substantially true for propellers. In reference 8 it is pointed out that, although the propellers of R. A. F. 6 section lost more in take-off efficiency owing to compressibility than those of Clark Y section, the efficiency at low tip speeds was higher; consequently, the efficiencies tended to equalize at high tip speeds.

CONCLUSIONS

1. The difference in maximum propulsive efficiency for propellers of different sections amounted to about 3 percent. The highest efficiencies were for the propeller sections of low mean cambers, as may be noted from the order of merit: N. A. C. A. 2400–34, Clark Y, N. A. C. A. $2R_200$, N. A. C. A. 4400, R. A. F. 6, and N. A. C. A. 6400.

2. The difference in take-off efficiency for controllable propellers varied from 2 to 8 percent, depending upon the section, the design C_s value, and the method of comparison. Based on propellers of the same diameter, the order of merit of the sections, in general, was: R. A. F. 6, N. A. C. A. 4400, Clark Y, N. A. C. A. 6400, N. A. C. A. $2R_200$, and N. A. C. A. 2400–34. Based on propellers of which the diameters were those giving maximum efficiency at high speed, the order of merit of the sections, in general, was: N. A. C. A. $2R_200$, Clark Y, N. A. C. A. 4400, N. A. C. A. 2400–34, R. A. F. 6, and N. A. C. A. 6400.

3. The difference in take-off efficiency for fixed-pitch propellers varied through wide limits. Based on either method of comparison, the order of merit was: R. A. F. 6 or N. A. C. A. 6400, N. A. C. A. 4400, Clark Y, N. A. C. A. $2R_200$, and N. A. C. A. 2400–34.

4. The tests indicated that blade sections for controllable propellers not limited in diameter should be selected almost entirely on a basis of minimum drag, as the maximum lift coefficients had only a small effect on the take-off characteristics within the range investigated, because the stall, in general, did not occur.

5. The tests indicated that blade sections for fixed-pitch propellers should be selected on bases of both minimum drag and maximum lift, particularly for blade-angle settings of 20° and over. For propellers of equal diameters, the increase in take-off thrust was proportional, in general, to the maximum lift.

6. A comparison of Clark Y and R. A. F. 6 sections of different thickness ratios for controllable propellers of the same diameter indicated that thin (h/b 0.07) propellers of R. A. F. 6 section were superior at take-off to thin propellers of Clark Y section, but that thick (h/b=0.09) propellers of Clark Y section were equal to those of R. A. F. 6 section, either thick or thin.

7. Tests already reported on the effect of compressibility indicate that no correction need be applied to the maximum efficiency of the present results for tip-speed values of V/V_c up to 0.80 or 0.90. Although corrections should be applied to the take-off characteristics for somewhat lower tip-speed values, the results show that compressibility tends to decrease any differences between propellers of different section. The present tests probably show the correct order of merit even up to tip speeds of $0.90V_c$.

LANGLEY MEMORIAL AERONAUTICAL LABORATORY,
NATIONAL ADVISORY COMMITTEE FOR AERONAUTICS,
LANGLEY FIELD, VA., *March 23, 1938.*

REFERENCES

1. Stack, John: The N. A. C. A. High-Speed Wind Tunnel and Tests of Six Propeller Sections. T. R. No. 463, N. A. C. A., 1933.
2. Freeman, Hugh B.: Comparison of Full-Scale Propellers Having R. A. F. 6 and Clark Y Airfoil Sections. T. R. No. 378, N. A. C. A., 1931.
3. Jacobs, Eastman N., Ward, Kenneth E., and Pinkerton, Robert M.: The Characteristics of 78 Related Airfoil Sections from Tests in the Variable-Density Wind Tunnel. T. R. No. 460, N. A. C. A., 1933.
4. Stack, John, and von Doenhoff, Albert E.: Tests of 16 Related Airfoils at High Speeds. T. R. No. 492, N. A. C. A., 1934.
5. Weick, Fred E., and Wood, Donald H.: The Twenty-Foot Propeller Research Tunnel of the National Advisory Committee for Aeronautics. T. R. No. 300, N. A. C. A., 1928.
6. Biermann, David, and Hartman, Edwin P.: Tests of Five Full-Scale Propellers in the Presence of a Radial and a Liquid-Cooled Engine Nacelle, Including Tests of Two Spinners. T. R. No. 642, N. A. C. A., 1938.
7. Lock, C. N. H.: A Graphical Method of Calculating the Performance of an Airscrew. R. & M. No. 1675, British A. R. C., 1935.
8. Biermann, David, and Hartman, Edwin P.: The Effect of Compressibility on Eight Full-Scale Propellers Operating in the Take-Off and Climbing Range. T. R. No. 639, N. A. C. A., 1938.
9. Wood, Donald H.: Full-Scale Tests of Metal Propellers at High Tip Speeds. T. R. No. 375, N. A. C. A., 1931.

TABLE II

CLARK Y AND R. A. F. 6 BASIC PROPELLER SECTIONS

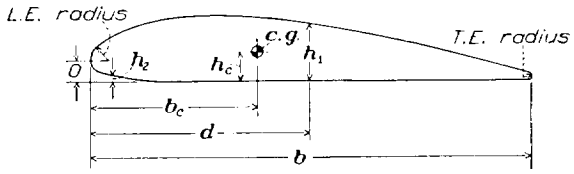

$h = h_{1_{max}}$

Section	Clark Y		R. A. F. 6
d/b	h_1/h	h_2/h	h_1/h
0	0.2950	0.2950	
.025	.5490	.1281	0.41
.05	.6625	.0811	.59
.1	.8055	.0384	.79
.2	.9570	.0085	.95
.3	.9950	0	1.00
.4	.9830	0	.99
.5	.9280	0	.95
.6	.8290	0	.87
.7	.6835	0	.74
.8	.5210	0	.56
.9	.3375	0	.35
L. E. radius	0.13		.10
T. E. radius	.08		.07
h_c	.416 h		.421 h
b_c	.4405 b		.4469 b
Area	.7245 bh		.738 bh
I_{major}	.0418 b^3h		.0446 b^3h
I_{minor}	.0454 bh^3		.0464 bh^3

TABLE III

N. A. C. A. BASIC PROPELLER SECTIONS

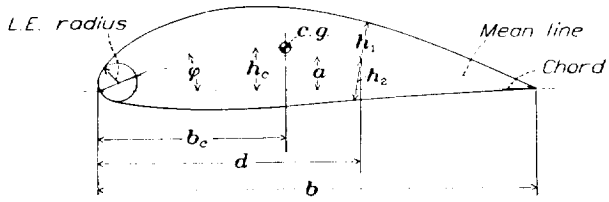

$(h_1 + h_2)_{max} = h$; h_1 and h_2 are measured perpendicular to the tangent of the mean line

Section	4400		2400 34		2R80		6400	
d/b	a/b	$h_1/h = h_2/h$	a/b	$h_1/h = h_2/h$	a/b	$h_1/h = h_2/h$	a/b	$h_1/h = h_2/h$
0.025	0.00184	0.2179	0.00242	0.140	0.00361	0.2179	0.00727	0.2179
.05	.00937	.2962	.00469	.208	.00681	.2962	.01406	.2962
.1	.01750	.3902	.00875	.304	.01204	.3902	.02625	.3902
.2	.03000	.4781	.01500	.425	.01833	.4781	.04500	.4781
.3	.03750	.5001	.01875	.484	.01999	.5001	.05625	.5001
.4	.04000	.4836	.02000	.500	.01821	.4836	.06000	.4836
.5	.03889	.4411	.01944	.486	.01414	.4411	.05834	.4411
.6	.03556	.3803	.01778	.443	.08930	.3803	.05333	.3803
.7	.03000	.3053	.01500	.373	.03710	.3053	.04501	.3053
.8	.02222	.2186	.01111	.277	−.00024	.2186	.03334	.2186
.9	.01222	.1206	.00611	.156	−.00187	.1206	.01834	.1206
1.0	0	.0105	0	.010	0	.0105	0	.0105
L. E. radius/b	1.1 $(h/b)^2$		0.275 $(h/b)^2$		1.1 $(h/b)^2$		1.1 $(h/b)^2$	
$\tan \varphi$	0.200		0.100		0.153		0.300	
b_c	.42b		.46b		.42b		.42b	
h_c	.0313b		.0172b		.0126b		.0473b	

TABLE IV

PERFORMANCE OF PROPELLERS HAVING DIAMETER FOR MAXIMUM EFFICIENCY AT HIGH SPEED

Propeller	Section	Design C_s	High speed				Take-off, controllable pitch			Take-off, fixed pitch				
			$\frac{V}{nD}$	Diameter (ft.)	Blade angle (deg.)	η_{max}	$\frac{V}{nD}$	Blade angle (deg.)	η	$\frac{V}{nD}$	Blade angle (deg.)	η	$\frac{N}{N_0}$	$\eta\left(\frac{N}{N_0}\right)$
5868-9	Clark Y	1.0	0.505	10	13.2	0.766	0.126	10.8	0.307	0.151	13.2	0.340	0.835	0.284
		1.5	.852	10	21.9	.848	.213	15.4	.428	.282	21.9	.411	.757	.311
		2.0	1.213	10	29.1	.861	.304	19.3	.500	.437	29.1	.397	.693	.275
		2.5	1.598	10	36.1	.850	.400	22.7	.548	.595	36.1	.403	.670	.270
5868-R6	R. A. F. 6	1.0	.553	9.14	16.4	.763	.138	13.9	.312	.157	16.4	.320	.877	.280
		1.5	.935	9.12	25.7	.830	.234	20.7	.400	.273	25.7	.384	.855	.328
		2.0	1.282	9.47	31.6	.843	.320	22.8	.480	.410	31.6	.419	.781	.327
		2.5	1.705	9.37	38.8	.828	.426	28.2	.521	.560	38.8	.390	.761	.297
6623-A	N. A. C. A. 4400	1.0	.553	9.14	16.4	.771	.138	13.9	.312	.157	16.4	.320	.878	.281
		1.5	.889	9.59	23.3	.837	.222	17.5	.415	.271	23.3	.401	.820	.329
		2.0	1.244	9.75	29.9	.848	.311	20.9	.492	.422	29.9	.392	.735	.289
		2.5	1.655	9.65	37.2	.832	.414	26.0	.521	.578	37.2	.387	.716	.277
6623-B	N. A. C. A. 4400 inner half, 2400-34 outer half.	1.0	.505	10.00	15.2	.786	.126	12.9	.338	.151	15.2	.334	.835	.279
		1.5	.830	10.27	22.8	.850	.207	16.1	.415	.282	22.8	.383	.734	.281
		2.0	1.154	10.51	28.8	.871	.289	18.4	.496	.438	28.8	.413	.659	.272
		2.5	1.545	10.34	36.4	.846	.386	22.7	.526	.601	36.4	.415	.638	.265
6623-C	N. A. C. A. $2R_2$00	1.0	.478	10.57	15.0	.776	.119	11.5	.329	.156	15.0	.349	.764	.267
		1.5	.788	10.81	21.8	.843	.197	14.6	.435	.282	21.8	.452	.698	.316
		2.0	1.168	10.40	30.0	.861	.292	20.0	.503	.448	30.0	.383	.651	.250
		2.5	1.582	10.10	38.3	.845	.396	24.8	.529	.626	38.3	.387	.630	.244
6623-D	N. A. C. A. 6400	1.0	.562	8.98	15.5	.747	.141	13.2	.303	.159	15.5	.307	.885	.272
		1.5	.905	9.41	22.4	.831	.226	16.6	.400	.274	22.4	.406	.826	.335
		2.0	1.282	9.47	29.4	.842	.320	20.7	.474	.396	29.4	.446	.809	.361
		2.5	1.705	9.37	37.4	.823	.426	26.8	.526	.562	37.4	404	.757	.308

TABLE V

PERFORMANCE OF PROPELLERS OF EQUAL DIAMETER

[Clark Y propeller taken as standard]

Propeller	Section	Design C_s	High speed				Take-off, controllable pitch			Take-off, fixed pitch				
			$\frac{V}{nD}$	Diameter (ft.)	Blade angle (deg.)	η_{max}	$\frac{V}{nD}$	Blade angle (deg.)	η	$\frac{V}{nD}$	Blade angle (deg.)	η	$\frac{N}{N_0}$	$\eta\left(\frac{N}{N_0}\right)$
5868-9	Clark Y	1.0	0.505	10	13.2	0.766	0.126	11.8	0.307	0.151	13.2	0.340	0.835	0.284
		1.5	.852	10	21.9	.848	.213	15.4	.428	.282	21.9	.411	.757	.311
		2.0	1.213	10	29.1	.861	.304	19.3	.500	.437	29.1	.397	.693	.275
		2.5	1.598	10	36.1	.850	.400	22.7	.548	.595	36.1	.403	.670	.270
5868-R6	R. A. F. 6	1.0	.505	10	12.5	.731	.126	10.8	.311	.145	12.5	.338	.869	.294
		1.5	.852	10	21.5	.816	.213	15.3	.428	.276	21.5	.449	.774	.347
		2.0	1.213	10	28.7	.833	.304	18.9	.508	.412	28.7	.491	.734	.361
		2.5	1.598	10	35.8	.817	.400	22.7	.570	.568	35.8	.474	.702	.333
6623-A	N. A. C. A. 4400	1.0	.505	10	13.4	.765	.126	10.8	.327	.154	13.4	.348	.820	.295
		1.5	.852	10	21.5	.835	.213	15.2	.428	.274	21.5	.430	.779	.335
		2.0	1.213	10	28.7	.844	.304	19.0	.508	.420	28.7	.427	.722	.308
		2.5	1.598	10	35.5	.832	.400	23.2	.560	.582	35.5	.420	.695	.292
6623-B	N. A. C. A. 4400 inner half, 2400-34 outer half.	1.0	.505	10	15.3	.786	.126	12.9	.338	.152	15.3	.332	.830	.276
		1.5	.852	10	23.9	.848	.213	17.3	.363	.287	23.9	.361	.743	.268
		2.0	1.213	10	31.0	.866	.304	21.1	.456	.436	31.0	.374	.694	.259
		2.5	1.598	10	37.8	.843	.400	24.6	.492	.600	37.8	.392	.665	.260
6623-C	N. A. C. $2R_2$00	1.0	.505	10	16.7	.745	.126	13.0	.319	.159	16.7	.337	.794	.264
		1.5	.852	10	24.7	.837	.213	18.1	.410	.291	24.7	.360	.731	.263
		2.0	1.213	10	31.8	.860	.304	21.9	.486	.445	31.8	.354	.680	.241
		2.5	1.598	10	38.7	.843	.400	25.3	.510	.625	38.7	.377	.637	.240
6623-D	N. A. C. A. 6400	1.0	.505	10	11.3	.731	.126	10.8	.319	.146	11.3	.337	.866	.292
		1.5	.852	10	19.6	.828	.213	13.7	.421	.278	19.6	.435	.766	.334
		2.0	1.213	10	26.9	.835	.304	17.0	.497	.405	26.9	.502	.747	.375
		2.5	1.598	10	33.9	.816	.400	20.6	.563	.557	33.9	.496	.715	.354

U. S. GOVERNMENT PRINTING OFFICE: 1939

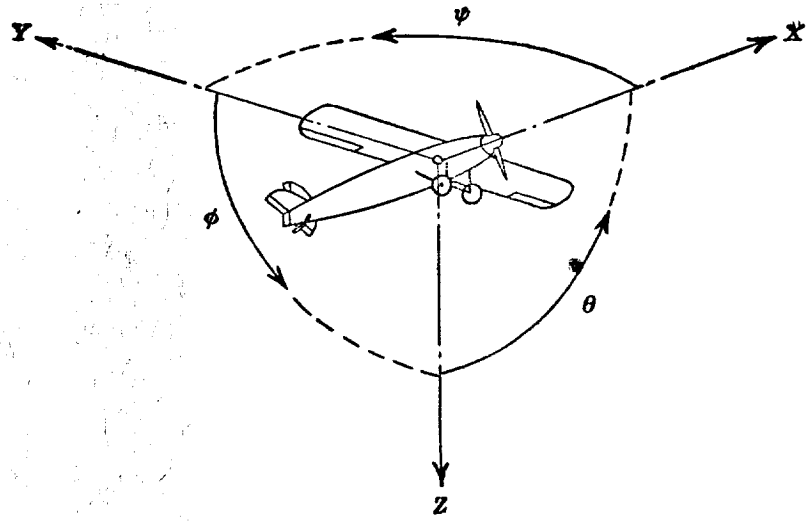

Positive directions of axes and angles (forces and moments) are shown by arrows

Axis		Force (parallel to axis) symbol	Moment about axis			Angle		Velocities	
Designation	Symbol		Designation	Symbol	Positive direction	Designation	Symbol	Linear (component along axis)	Angular
Longitudinal	X	X	Rolling	L	$Y \longrightarrow Z$	Roll	ϕ	u	p
Lateral	Y	Y	Pitching	M	$Z \longrightarrow X$	Pitch	θ	v	q
Normal	Z	Z	Yawing	N	$X \longrightarrow Y$	Yaw	ψ	w	r

Absolute coefficients of moment

$C_l = \frac{L}{qbS}$ (rolling) $\quad C_m = \frac{M}{qcS}$ (pitching) $\quad C_n = \frac{N}{qbS}$ (yawing)

Angle of set of control surface (relative to neutral position), δ. (Indicate surface by proper subscript.)

4. PROPELLER SYMBOLS

D, Diameter

p, Geometric pitch

p/D, Pitch ratio

V', Inflow velocity

V_s, Slipstream velocity

T, Thrust, absolute coefficient $C_T = \frac{T}{\rho n^2 D^4}$

Q, Torque, absolute coefficient $C_Q = \frac{Q}{\rho n^2 D^5}$

P, Power, absolute coefficient $C_P = \frac{P}{\rho n^3 D^5}$

C_s, Speed-power coefficient $= \sqrt[5]{\frac{\rho V^5}{P n^2}}$

η, Efficiency

n, Revolutions per second, r.p.s.

Φ, Effective helix angle $= \tan^{-1}\left(\frac{V}{2\pi r n}\right)$

5. NUMERICAL RELATIONS

1 hp. = 76.04 kg-m/s = 550 ft-lb./sec.
1 metric horsepower = 1.0132 hp.
1 m.p.h. = 0.4470 m.p.s.
1 m.p.s. = 2.2369 m.p.h.

1 lb. = 0.4536 kg.
1 kg = 2.2046 lb.
1 mi. = 1,609.35 m = 5,280 ft.
1 m = 3.2808 ft.

NATIONAL ADVISORY COMMITTEE

FOR AERONAUTICS

T A B L E S I - VI

Supplement
to

REPORT NO. 650

THE AERODYNAMIC CHARACTERISTICS OF SIX FULL-SCALE PROPELLERS HAVING DIFFERENT AIRFOIL SECTIONS

By David Biermann and Edwin P. Hartman

1939

TABLE I

PROPELLER 5868-9

Values of C_T

V/nD	Blade angle at 0.75R (deg.) 15	20	25	30	35	40	45
0.2	0.1172						
.3	.1010	0.1400		0.1608			
.4	.0835	.1262	0.1520	.1581	0.1662	0.1719	0.1852
.5	.0647	.1108	.1465	.1538	.1618	.1695	.1878
.6	.0455	.0928	.1350	.1533	.1590	.1665	.1875
.7	.0257	.0730	.1198	.1510	.1568	.1625	.1840
.8	.0031	.0524	.1009	.1432	.1544	.1578	.1783
.9		.0306	.0812	.1288	.1527	.1510	.1723
1.0		.0087	.0607	.1122	.1455	.1466	.1671
1.1			.0388	.0925	.1342	.1472	.1630
1.2			.0177	.0720	.1179	.1459	.1595
1.3				.0516	.1004	.1403	.1581
1.4				.0309	.0820	.1297	.1580
1.5				.0100	.0633	.1143	.1578
1.6					.0450	.0980	.1529
1.7					.0262	.0811	.1418
1.8					.0058	.0644	.1282
1.9						.0479	.1140
2.0						.0315	.0997
2.1						.0148	.0854
2.2							.0709
2.3							.0560
2.4							.0395
2.5							.0228
2.6							.0069

Values of C_P

V/nD	Blade angle at 0.75R (deg.) 15	20	25	30	35	40	45
0.2	0.0572						
.3	.0546	0.0869		0.1900			
.4	.0503	.0849	0.1268	.1832	0.2378	0.2972	0.3901
.5	.0433	.0811	.1225	.1763	.2300	.2920	.3873
.6	.0340	.0738	.1178	.1707	.2230	.2854	.3823
.7	.0224	.0631	.1110	.1650	.2160	.2779	.3749
.8	.0067	.0498	.1007	.1570	.2099	.2693	.3657
.9		.0326	.0870	.1482	.2060	.2600	.3554
1.0		.0132	.0709	.1372	.1982	.2508	.3465
1.1			.0503	.1201	.1879	.2492	.3385
1.2			.0272	.1002	.1744	.2473	.3327
1.3				.0783	.1567	.2398	.3287
1.4				.0520	.1352	.2269	.3263
1.5				.0230	.1112	.2095	.3252
1.6					.0855	.1874	.3180
1.7					.0583	.1631	.3028
1.8					.0257	.1380	.2820
1.9						.1125	.2610
2.0						.0860	.2402
2.1						.0573	.2164
2.2							.1940
2.3							.1700
2.4							.1380
2.5							.0992
2.6							.0579

Values of η

V/nD	Blade angle at 0.75R (deg.) 15	20	25	30	35	40	45
0.2	0.410						
.3	.555	0.483		0.254			
.4	.664	.595	0.479	.345	0.280	0.231	0.190
.5	.747	.683	.598	.435	.352	.290	.242
.6	.803	.754	.587	.538	.428	.350	.294
.7	.803	.810	.756	.640	.508	.410	.344
.8	.370	.842	.802	.730	.588	.469	.390
.9		.844	.839	.782	.667	.523	.436
1.0		.659	.857	.818	.734	.585	.482
1.1			.850	.846	.786	.650	.530
1.2			.782	.862	.811	.708	.575
1.3				.857	.832	.761	.626
1.4				.832	.849	.801	.678
1.5				.652	.854	.818	.728
1.6					.842	.837	.769
1.7					.764	.845	.796
1.8					.406	.840	.818
1.9						.809	.830
2.0						.733	.830
2.1						.542	.828
2.2							.804
2.3							.758
2.4							.688
2.5							.575
2.6							.310

Values of C_s

V/nD	Blade angle at 0.75R (deg.) 15	20	25	30	35	40	45
0.2	0.355						
.3	.537	0.489		0.418			
.4	.727	.655	0.604	.562	0.533	0.509	0.483
.5	.936	.826	.761	.707	.671	.639	.604
.6	1.178	1.010	.920	.855	.810	.771	.728
.7	1.496	1.217	1.087	1.004	.951	.904	.852
.8	2.180	1.457	1.266	1.157	1.093	1.040	.978
.9		1.786	1.468	1.318	1.235	1.178	1.106
1.0		2.376	1.698	1.488	1.382	1.319	1.236
1.1			2.000	1.682	1.536	1.452	1.365
1.2			2.464	1.903	1.702	1.587	1.496
1.3				2.166	1.885	1.729	1.623
1.4				2.532	2.090	1.885	1.751
1.5				3.191	2.326	2.050	1.876
1.6					2.620	2.238	2.012
1.7					3.003	2.440	2.160
1.8					3.742	2.673	2.320
1.9						2.940	2.486
2.0						3.272	2.660
2.1						3.723	2.851
2.2							3.055
2.3							3.275
2.4							3.563
2.5							3.970
2.6							4.600

TABLE II

PROPELLER 5868-R6

$\frac{V}{nD}$	Values of C_T						Values of C_P					
	Blade angle at 0.75R (deg.)						Blade angle at 0.75R (deg.)					
	15	20	25	30	35	40	15	20	25	30	35	40
0.2						0.1776	0.0569	0.0885	0.1232			0.2868
.3	0.1055	0.1468	0.1790			.1766	.0530	.0870	.1229	0.1620	0.2162	.2831
.4	.0884	.1312	.1676	0.1826	0.1762	.1764	.0467	.0830	.1225	.1638	.2098	.2765
.5	.0697	.1140	.1541	.1817	.1784	.1770	.0380	.0761	.1193	.1656	.2029	.2696
.6	.0491	.0958	.1387	.1780	.1798	.1763	.0273	.0666	.1131	.1651	.2024	.2638
.7	.0284	.0758	.1218	.1661	.1784	.1801	.0155	.0538	.1040	.1609	.2049	.2598
.8	.0058	.0547	.1037	.1517	.1772	.1806		.0390	.0914	.1527	.2041	.2588
.9		.0335	.0840	.1347	.1682	.1801		.0231	.0755	.1405	.2010	.2600
1.0		.0118	.0630	.1157	.1560	.1800			.0573	.1258	.1918	.2658
1.1			.0425	.0959	.1400	.1742			.0368	.1063	.1771	.2664
1.2			.0215	.0747	.1218	.1576				.0845	.1590	.2544
1.3				.0541	.1027	.1403				.0612	.1385	.2385
1.4				.0336	.0836	.1228				.0370	.1161	.2202
1.5				.0120	.0648	.1053					.0927	.2008
1.6					.0464	.0881					.0679	.1785
1.7					.0276	.0709					.0377	.1550
1.8					.0080	.0537						.1285
1.9						.0367						.1023
2.0						.0195						.0750
2.1						.0017						.0424
2.2												

$\frac{V}{nD}$	Values of η						Values of C_s					
	Blade angle at 0.75R (deg.)						Blade angle at 0.75R (deg.)					
	15	20	25	30	35	40	15	20	25	30	35	40
0.2						0.186	0.533	0.498	0.456			0.385
.3	0.556	0.497	0.436			.249	.721	.652	.608	0.575	0.543	.515
.4	.668	.604	.546	0.451	0.326	.319	.923	.824	.761	.718	.683	.647
.5	.747	.687	.629	.554	.425	.395	1.154	1.005	.918	.860	.825	.780
.6	.776	.755	.697	.645	.532	.473	1.437	1.202	1.082	1.003	.963	.914
.7	.728	.797	.754	.704	.616	.555	1.840	1.435	1.258	1.153	1.098	1.047
.8	.299	.813	.797	.754	.692	.627		1.721	1.454	1.310	1.236	1.180
.9		.773	.827	.794	.741	.692		2.128	1.675	1.482	1.378	1.310
1.0		.510	.834	.824	.776	.746			1.951	1.665	1.530	1.436
1.1			.816	.838	.803	.784			2.321	1.878	1.698	1.564
1.2			.701	.843	.826	.806				2.133	1.879	1.710
1.3				.832	.840	.824				2.447	2.081	1.867
1.4				.769	.845	.834				2.900	2.308	.203
1.5				.487	.838	.839					2.577	.221
1.6					.801	.839					2.912	.240
1.7					.692	.824					3.467	.261
1.8					.382	.794						.287
1.9						.717						.315
2.0						.546						.352
2.1						.088						.414
2.2												

TABLE III

PROPELLER 6823-A

Values of C_T

$\frac{V}{nD}$	Blade angle at 0.75R (deg.)					
	15	20	25	30	35	40
0.2						0.1761
.3	0.1058	0.1447	0.1636			.1755
.4	.0895	.1314	.1570	0.1613	0.1718	.1738
.5	.0712	.1172	.1480	.1618	.1666	.1712
.6	.0509	.0999	.1360	.1639	.1609	.1685
.7	.0299	.0799	.1213	.1585	.1587	.1656
.8	.0078	.0581	.1043	.1468	.1608	.1620
.9		.0355	.0852	.1330	.1604	.1583
1.0		.0130	.0642	.1166	.1528	.1577
1.1			.0425	.0974	.1403	.1608
1.2			.0205	.0766	.1248	.1595
1.3				.0556	.1069	.1493
1.4				.0343	.0879	.1351
1.5				.0129	.0689	.1190
1.6					.0500	.1031
1.7					.0308	.0865
1.8					.0120	.0702
1.9						.0535
2.0						.0370
2.1						.0204
2.2						.0034

Values of C_P

$\frac{V}{nD}$	Blade angle at 0.75R (deg.)					
	15	20	25	30	35	40
0.2						0.3087
.3	0.0571	0.0884	0.1198			.2986
.4	.0535	.0875	.1172	0.1764	0.2335	.2896
.5	.0475	.0852	.1178	.1683	.2260	.2820
.6	.0386	.0789	.1171	.1613	.2190	.2755
.7	.0262	.0693	.1128	.1592	.2122	.2731
.8	.0110	.0560	.1045	.1566	.2061	.2687
.9		.0390	.0922	.1517	.2005	.2608
1.0		.0186	.0762	.1423	.1972	.2565
1.1			.0560	.1281	.1920	.2533
1.2			.0330	.1086	.1823	.2490
1.3				.0855	.1669	.2432
1.4				.0599	.1458	.2334
1.5				.0318	.1227	.2177
1.6					.0970	.1988
1.7					.0695	.1770
1.8					.0390	.1535
1.9						.1270
2.0						.0990
2.1						.0697
2.2						.0410

Values of η

$\frac{V}{nD}$	Blade angle at 0.75R (deg.)					
	15	20	25	30	35	40
0.2						
.3	0.556	0.491	0.410			
.4	.669	.600	.535	0.366	0.294	0.240
.5	.749	.688	.628	.480	.369	.304
.6	.791	.760	.697	.609	.441	.366
.7	.799	.807	.753	.697	.523	.424
.8	.567	.830	.798	.749	.624	.482
.9		.819	.832	.789	.720	.546
1.0		.699	.843	.820	.774	.615
1.1			.835	.836	.804	.698
1.2			.746	.846	.821	.769
1.3				.846	.833	.798
1.4				.802	.844	.810
1.5				.608	.842	.821
1.6					.825	.830
1.7					.753	.831
1.8					.554	.823
1.9						.801
2.0						.748
2.1						.615
2.2						.783

Values of C_s

$\frac{V}{nD}$	Blade angle at 0.75R (deg.)					
	15	20	25	30	35	40
0.2						
.3	0.532	0.488	0.459			
.4	.719	.651	.614	0.566	0.535	0.513
.5	.919	.820	.767	.714	.673	.644
.6	1.150	.998	.921	.864	.813	.776
.7	1.450	1.195	1.084	1.012	.955	.908
.8	1.971	1.426	1.256	1.160	1.097	1.040
.9		1.720	1.452	1.312	1.242	1.178
1.0		2.217	1.675	1.477	1.383	1.312
1.1			1.960	1.660	1.530	1.447
1.2			2.372	1.872	1.688	1.585
1.3				2.128	1.860	1.726
1.4				2.460	2.059	1.873
1.5				2.990	2.282	2.035
1.6					2.550	2.210
1.7					2.895	2.404
1.8					3.440	2.620
1.9						2.870
2.0						3.178
2.1						3.577
2.2						4.165

TABLE IV

PROPELLER 6623-B

$\frac{V}{nD}$	Values of C_T						Values of C_P					
	Blade angle at 0.75 R., deg.						Blade angle at 0.75 R., deg.					
	15	20	25	30	35	40	15	20	25	30	35	40
0.2	0.0977						0.0455					
.3	.0859	0.1177	0.1360	**0.1494**	0.1645		.0440	0.0733	0.1188	**0.1668**	0.2225	
.4	.0694	.1057	.1318	**.1446**	.1594	0.1730	.0390	.0691	.1100	**.1618**	.2164	0.2844
.5	.0492	.0904	.1232	.1393	.1540	.1692	.0313	.0636	.1022	.1559	.2099	.2772
.6	.0289	.0730	.1102	.1335	.1477	.1644	.0214	.0564	.0942	.1490	.2025	.2701
.7	.0083	.0540	.0957	.1272	.1403	.1568	.0090	.0455	.0858	.1402	.1950	.2633
.8		.0326	.0791	.1183	.1340	.1523		.0311	.0767	.1300	.1880	.2561
.9		.0107	.0614	.1040	.1291	.1463		.0135	.0648	**.1187**	.1810	.2489
1.0			.0409	.0879	.1227	.1402			.0471	.1060	.1709	.2415
1.1			.0192	.0705	.1123	.1347			.0262	.0905	.1577	.2342
1.2				.0521	.0989	.1299				.0722	.1428	.2258
1.3				.0330	.0812	.1225				.0506	.1237	.2121
1.4				.0174	.0621	.1118				.0252	.1011	.1953
1.5					.0426	.0978					.0759	.1768
1.6					.0228	.0822					.0480	.1561
1.7					.0029	.0650					.0190	.1319
1.8						.0471						.1046
1.9						.0294						.0757
2.0						.0113						.0457

$\frac{V}{nD}$	Values of η						Values of C_s					
	Blade angle at 0.75 R., deg.						Blade angle at 0.75 R., deg.					
	15	20	25	30	35	40	15	20	25	30	35	40
0.2	0.429						0.371					
.3	.586	0.482	0.343	0.269	0.222		.561	0.506	0.459	0.429	0.405	
.4	.712	.612	.479	.358	.294	0.243	.765	.683	.622	.575	.543	0.514
.5	.786	.711	.602	.447	.367	.305	1.000	.868	.788	.726	.683	.646
.6	.810	.777	.702	.538	.438	.365	1.067	1.067	.963	.878	.825	.779
.7	.646	.831	.780	.635	.503	.422	1.293	1.300	1.146	1.037	.971	.913
.8		.839	.825	.728	.570	.475	1.795	1.604	1.337	1.203	1.117	1.050
.9		.708	.853	.788	.642	.529		2.128	1.557	1.378	1.267	1.188
1.0			.868	.830	.718	.580			1.841	1.567	1.425	1.328
1.1			.806	.857	.783	.632			2.277	1.780	1.592	1.471
1.2				.867	.831	.690				2.030	1.773	1.615
1.3				.848	.853	.750				2.358	1.973	1.773
1.4				.634	.860	.801				2.923	2.215	1.942
1.5					.842	.830					2.517	2.122
1.6					.760	.842					2.937	2.318
1.7					.260	.838					3.751	2.548
1.8						.810						2.825
1.9						.738						3.183
2.0						.495						3.704

TABLE V

PROPELLER 6623-C

$\frac{V}{nD}$	Values of C_T						Values of C_P					
	Blade angle at 0.75 R., deg.						Blade angle at 0.75 R., deg.					
	15	20	25	30	35	40	15	20	25	30	35	40
0.2	0.0902	0.1287			0.1610	0.1720	0.0418	0.0691			0.2300	0.3005
.3	.0741	.1175	0.1373	0.1441	.1576	.1717	.0379	.0682	0.1139	0.1662	.2241	.2979
.4	.0560	.1030	.1353	.1386	.1534	.1707	.0320	.0655	.1025	.1625	.2170	.2945
.5	.0360	.0855	.1262	.1358	.1487	.1686	.0231	.0600	.0978	.1572	.2085	.2904
.6	.0154	.0657	.1113	.1357	.1431	.1649	.0124	.0503	.0932	.1496	.1992	.2852
.7		.0443	.0923	.1330	.1373	.1587		.0373	.0844	.1379	.1892	.2783
.8		.0224	.0722	.1202	.1339	.1522		.0219	.0711	.1271	.1820	.2684
.9		.0009	.0506	.1038	.1338	.1460		.0047	.0537	.1164	.1760	.2496
1.0			.0289	.0850	.1279	.1401			.0340	.1018	.1671	.2354
1.1			.0069	.0647	.1130	.1366			.0127	.0830	.1535	.2280
1.2				.0431	.0932	.1369				.0605	.1337	.2227
1.3				.0207	.0727	.1312				.0340	.1108	.2102
1.4					.0515	.1125					.0846	.1887
1.5					.0302	.0930					.0558	.1640
1.6					.0100	.0733					.0264	.1376
1.7						.0537						.1098
1.8						.0340						.0790
1.9						.0123						.0440

$\frac{V}{nD}$	Values of η						Values of C_s					
	Blade angle at 0.75 R., deg.						Blade angle at 0.75 R., deg.					
	15	20	25	30	35	40	15	20	25	30	35	40
0.2	0.432	0.373			0.140	0.115	0.378	0.341			0.268	0.254
.3	.587	.517	0.362	0.260	.211	.173	.576	.513	0.463	0.430	.405	.382
.4	.700	.629	.528	.341	.283	.232	.796	.690	.631	.575	.542	.511
.5	.779	.712	.646	.432	.357	.290	1.064	.879	.796	.724	.684	.640
.6	.745	.784	.716	.544	.431	.347	1.446	1.091	.965	.877	.829	.771
.7		.831	.765	.675	.508	.399		1.352	1.149	1.040	.976	.904
.8		.818	.812	.756	.588	.454		1.717	1.358	1.208	1.125	1.040
.9		.172	.848	.803	.685	.526		2.632	1.615	1.385	1.275	1.187
1.0			.851	.835	.765	.595			1.965	1.580	1.430	1.335
1.1			.600	.857	.810	.659			2.637	1.812	1.601	1.478
1.2				.855	.837	.738				2.105	1.793	1.620
1.3				.791	.853	.811				2.555	2.018	1.776
1.4					.853	.835					2.299	1.956
1.5					.812	.850					2.673	2.152
1.6					.607	.852					3.305	2.377
1.7						.832						2.644
1.8						.775						2.992
1.9						.531						3.550

TABLE VI

PROPELLER 6623-D

$\frac{V}{nD}$	Values of C_T						Values of C_P					
	Blade angle at 0.75 R., deg.						Blade angle at 0.75 R., deg.					
	15	20	25	30	35	40	15	20	25	30	35	40
0.2		0.1673	0.1873	0.1799	0.1886	0.1957		0.1034	0.1260	0.1708	0.2510	0.3040
.3	0.1173	.1588	.1831	.1840	.1860	.1930	0.0673	.1037	.1300	.1700	.2457	.3015
.4	.1011	.1475	.1769	.1875	.1841	.1907	.0638	.1029	.1343	.1694	.2384	.2982
.5	.0829	.1326	.1673	.1874	.1838	.1886	.0580	.1003	.1377	.1703	.2267	.2941
.6	.0631	.1148	.1546	.1830	.1875	.1872	.0493	.0948	.1381	.1738	.2180	.2895
.7	.0421	.0956	.1388	1751	.1918	.1859	.0371	.0857	.1342	.1772	.2149	.2841
.8	.0171	.0748	.1210	.1645	.1883	.1862	.0242	.0730	.1260	.1792	.2165	.2797
.9		.0528	.1008	.1505	.1816	.1920		.0573	.1124	.1767	.2213	.2773
1.0		.0295	.0798	.1339	.1727	.1935		.0387	.0959	.1665	.2240	.2767
1.1		.0022	.0590	.1156	.1610	.1868		.0187	.0773	.1538	.2221	.2780
1.2			.0382	.0957	.1458	.1828			.0562	.1370	.2144	.2825
1.3			.0153	.0752	.1272	.1755			.0325	.1161	.2002	.2863
1.4				.0541	.1072	.1597				.0912	.1799	.2781
1.5				.0323	.0867	.1406				.0633	.1557	.2583
1.6				.0099	.0666	.1208				.0350	.1283	.2350
1.7					.0461	.1013					.1000	.2089
1.8					.0253	.0817					.0714	.1803
1.9					.0043	.0620					.0419	.1498
2.0						.0421						.1175
2.1						.0222						.0845
2.2						.0022						.0515

$\frac{V}{nD}$	Values of η						Values of C_s					
	Blade angle at 0.75 R., deg.						Blade angle at 0.75 R., deg.					
	15	20	25	30	35	40	15	20	25	30	35	40
0.2			0.297	0.211	0.150	0.129			0.302	0.285	0.264	0.254
.3	0.523	0.459	.422	.325	.227	.192	0.515	0.472	.451	.427	.397	.381
.4	.634	.574	.527	.443	.309	.256	.693	.630	.598	.571	.532	.510
.5	.715	.662	.607	.550	.405	.321	.885	.792	.743	.712	.673	.638
.6	.768	.726	.672	.632	.516	.388	1.095	.962	.891	.851	.814	.769
.7	.794	.781	.724	.691	.625	.458	1.352	1.146	1.046	.990	.952	.901
.8	.565	.818	.768	.734	.696	.533	1.685	1.351	1.210	1.128	1.087	1.032
.9		.829	.807	.766	.738	.623		1.596	1.393	1.272	1.216	1.163
1.0		.763	.832	.804	.771	.699		1.916	1.600	1.430	1.348	1.294
1.1		.129	.840	.827	.797	.740		2.440	1.836	1.599	1.487	1.421
1.2			.816	.838	.816	.777			2.135	1.786	1.632	1.545
1.3			.612	.842	.826	.797			2.580	2.000	1.794	1.669
1.4				.831	.834	.805				2.262	1.972	1.809
1.5				.765	.836	.816				2.604	2.177	1.966
1.6				.453	.831	.822				3.125	2.413	2.136
1.7					.784	.824					2.694	2.325
1.8					.638	.816					3.051	2.533
1.9					.195	.786					3.585	2.780
2.0						.717						3.070
2.1						.552						3.448
2.2						.094						3.978